AN ABSTRACT OF THE THESIS OF

Sarah Aly Ahmed for the degree of Master of Science in Electrical and Computer Engineering presented on March 19, 2020.

Title: Hybrid AOA and TDOA Solution for Transmitter Positioning

Abstract approved: _____

Huaping Liu

Accurate positioning has become an active research area in recent years. It has a wide range of applications in many fields such as navigation, asset tracking, health care, proximity marketing/location-based advertising, and sport analytics. Transmitter positioning via radio frequency (RF) signals is the most widely encountered scenario, and it uses a two-step process: First, parameters that depend on the location of the transmitter are extracted from the received signal. Second, the transmitter's location is estimated by using these parameters. Many parameters can be used; for instance, time of arrival (TOA), time difference of arrival (TDOA), angle of arrival (AOA), and received signal strength (RSS). Localization can use one or multiple of such parameters. In this thesis, a hybrid AOA and TDOA method is studied. Specifically, an array of N collinear receiving antennas are employed to estimate the transmitter position. In order to use AOA, existing assumes that the transmitter is far away from the receiving antennas and that the spacing between the receiving antennas is very small (typically a fraction of one wavelength). This ensures that the directions of the incident waves to all receivers are parallel, so that there is a single AOA for all receivers. Such condition cannot be maintained for some scenarios (e.g., when wavelength is very large). Also, in order to use valid TDOAs, the receiving antennas cannot be placed very close to one another, which will result a unique AOA for each of the receiving antennas. This research develop solutions for the cases where the above constraints cannot be maintained. A maximum likelihood (ML) estimator is developed to obtain the AOA of each receiving antenna assuming there is no limitation on the antenna spacing; it can be sufficiently large or

small . A cross correlation algorithm is used to determine the TDOA between the received signals. Finally, an algorithm that jointly processes the AOAs and the TDOAs to estimate the position of the transmitter is developed.

Hybrid AOA and TDOA Solution for Transmitter Positioning

by

Sarah Aly Ahmed

A THESIS

submitted to

Oregon State University

in partial fulfillment of
the requirements for the
degree of

Master of Science

Presented March 19, 2020
Commencement June 2020

Master of Science thesis of Sarah Aly Ahmed presented on March 19, 2020.

APPROVED:

Major Professor, representing Electrical and Computer Engineering

---

Director of the School of Electrical Engineering and Computer Science

---

Dean of the Graduate School

I understand that my thesis will become part of the permanent collection of Oregon State University libraries. My signature below authorizes release of my thesis to any reader upon request.

Sarah Aly Ahmed, Author

ACKNOWLEDGEMENTS

I would like to thank my parents for whom I owe everything. I also would like to thank my husband for his help and support. I would have never completed my graduate research without his encouragement. I thank the committee and a special thanks for Prof. Liu for his guidance throughout the research. A very special thanks to Prof. Raich for his advice during the research. Finally, I want to thank my colleagues Tingwei Zhang and Guangxin Wang for their help throughout my graduate research.

TABLE OF CONTENTS

LIST OF FIGURES

LIST OF FIGURES (Continued)

Figure Page

LIST OF FIGURES (Continued)

Figure Page

LIST OF ALGORITHMS

Algorithm Page

Chapter 1: Introduction

1.1 Problem Statement

Transmitter positioning [1–8] has become one of the most widely studied research areas due to its vast applications in many fields such as, navigation, asset tracking, health care, proximity marketing/location-based advertising, and sport analytics. Positioning via radio frequency (RF) signals is the most commonly encountered scenario and it uses a two-step process. First, some parameters are extracted from the received signals at each anchor point (which is assumed to be a receiver in this thesis). These parameters can be time-of-arrival (TOA), time-difference-of-arrival (TDOA), angle-of-arrival (AOA) and received signal strength (RSS) information. In AOA system, the anchor antennas are typically assumed to be closely placed (typically a fraction of one wavelength) and the transmitter is very far from them such that the incident signals are parallel to all receive antennas; i.e., all receiving antennas have the same AOA [9–13]. This assumption has many limitations in some application scenarios. One scenario that we consider here is to use both AOA and TDOA information, but from a single array of receivers, aiming to generate the simplest system. In this case the antennas cannot be placed closely to be able to detect the time delay between the incident signals at each receiver. This is because when the receiving antennas are placed very close together (e.g., a fraction of a meter), it is difficult to derive from these antennas any meaningful TDOA values, since even with ultrawideband signaling [14–23], it is difficult to obtain decimeter-level-

accurate TDOAs. Accordingly the angles of arrival are no longer equal. Existing work has used different anchors to combine TDOA and AOA, which require at least three anchors for 2D positioning. In such cases, the AOA is mainly used for increasing the accuracy, but the system is as complex as a conventional TDOA system.

1.2 Proposed Scheme

The research in this thesis aims to design a very simple system: using a single linear array of N receivers each with one antenna for 2D positioning under the condition that the transmitter is on one side of the array. Of course in this system the same anchor (i.e., the array of receivers) can be used for AOA positioning, for TDOA positioning, or for positioning using both TDOA and AOA. All three approaches are analyzed and studied in this thesis. To be able to use the same array, an algorithm that does not restrict the receiving antennas to be very closely placed together is developed. This system can thus be used for 'near field' positioning scenario, i.e., the transmitter can be close to the anchor, since it does not assume that the signal from the transmitter have the same AOA to all the receivers on the array. To make the analysis simple, N co-linear receiving antennas are placed equidistant from one another with a distance d. The performance of this system does not change if the parameter d equals an integer multiple of the wavelength λ. We will analyze the mean squared error (MSE) performance of this system as a function of the signal-to-noise ratio (SNR) for the three cases mentioned above: AOA, TDOA, and a hybrid approach.

1.3 Thesis Organization

The thesis is organized as follows. Chapter 2 reviews existing AOA solutions based on the 'far field' assumption. It also includes a review of the polygon area oriented systems along with the results for these approaches as well as hybrid TDOA and AOA solutions and how the individual results are used together to estimate the transmitter location.

Chapter 3 presents the proposed system architecture, transmitter and receiver arrangement, also explains the transmitter specifications along with the channel modeling. It also develops an analytical solution of the algorithms used in each of the the three approaches: AOA estimation approach, TDOA estimation approach, and the hybrid TDOA/AOA estimation approach.

Chapter 4 presents simulation results that include the properties of the signal transmitted and channel implemented for each of the implemented approaches. Performance in terms of the MSE versus SNR is presented for each approach.

Chapter 5 provides a summary of the work and outlines a few areas of work that could be done in the future.

Chapter 2: Related Work

This chapter reviews related work for AOA and TDOA approaches. It also sumamrizes how their results can be used in this research to create a hybrid solution, which is very simple to deploy while still maintaining a good performance.

The conventional way of estimating the TDOA, as explained in [9–11, 29], uses cross-correlation of the received signals at multiple sensors (anchor). One of the receivers may be assumed to be a reference anchor (i.e., the time of arrival of the received signal at this anchor equals zero). The time instants of the received signals at the rest of the anchors are compared with that of the reference anchor.

Let us use the example of 2 receivers as shown in Fig. 2.1. This difference in distance travelled can be used to calculate the time difference of arrival using the two equations below, assuming that A is the reference receiver, X_A , Y_A ,X_B ,Y_B ,X_C and Y_C are the coordinates of the receivers, and X_T and Y_T are the unknown coordinates of the transmitter.

$$d_{AB} = \sqrt{(X_A - X_T)^2 + (Y_A - Y_T)^2} - \sqrt{(X_B - X_T)^2 + (Y_B - Y_T)^2} \tag{2.1}$$

$$d_{AC} = \sqrt{(X_A - X_T)^2 + (Y_A - Y_T)^2} - \sqrt{(X_C - X_T)^2 + (Y_C - Y_T)^2}. \tag{2.2}$$

The time difference of arrival can be calculated using the relationship:

$$\tau_{AB} = \frac{d_{AB}}{u} \tag{2.3}$$

$$\tau_{AC} = \frac{d_{AC}}{u}, \tag{2.4}$$

where u is the speed of light in vacuum.

Solving equations (2.1) and (2.2) simultaneously yields the transmitter position. In other words, in the ideal case, the hyperbolas represented by equations (2.1) and (2.2) intersect at the transmitter position.

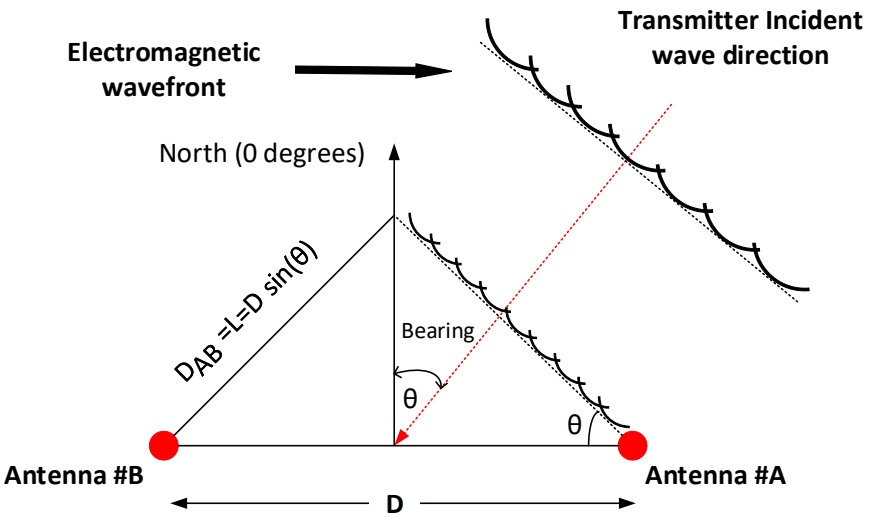

Figure 2.1: Interferometry technologies applied in AOA monitoring station configured a pair of closely spaced antenna at the same monitoring station.

The conventional way of estimating angle of arrival can be found in [9–11]. The spacing between the receivers is typically small (e.g., half a wavelength) and the transmitter

placed far away from the antenna array. Thus, all incident waves are approximately parallel, and all receivers have almost the same angle of arrival, as illustrated in Fig. 2.1. Angle of arrival can be estimated using the phase difference between the received signals as

$$\Delta\phi = 2\ \pi\ D \sin(\theta)\ \frac{f}{u}. \tag{2.5}$$

2.1 Time Difference of Arrival Estimation

The cross correlation algorithm is a good way to estimate the time difference as it can deal with cases with an unknown transmission time and unknown transmitted signal.

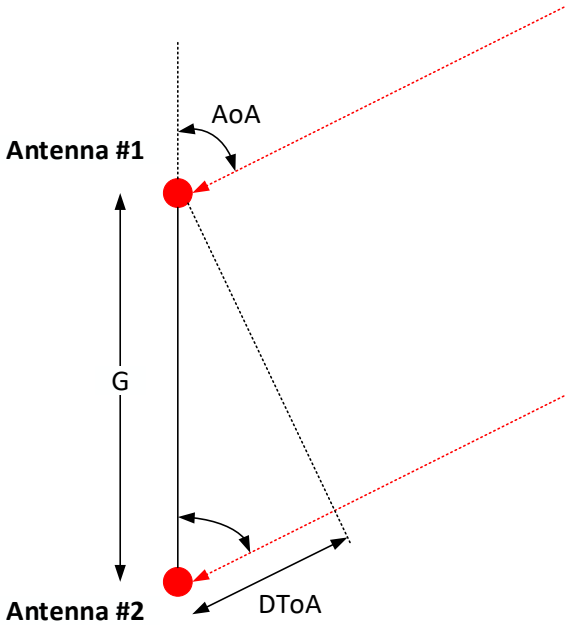

Figure 2.2: Illustration of parallel incident waves.

In [24], the antennas have a spacing that is much smaller than the distance from the transmitter; thus the incident rays are assumed to be parallel as illustrated in Fig. 2.2. The time difference between the received signals can be written as

$$\tau_D = G \times \frac{\cos(AOA)}{u}. \tag{2.6}$$

This puts a limitation on the maximum value of τ_D to be

$$\tau_D = \frac{G}{u}. \tag{2.7}$$

Obtaining the TDOA typically requires two steps: first, obtaining the cross-correlation points, and second, quadratic interpolation of these estimated points. Cross-correlation is commonly done via the complex baseband filtering (to extract the in-phase (I) and quadrature (Q) components). The system model for this approach is shown in Fig. 2.3.

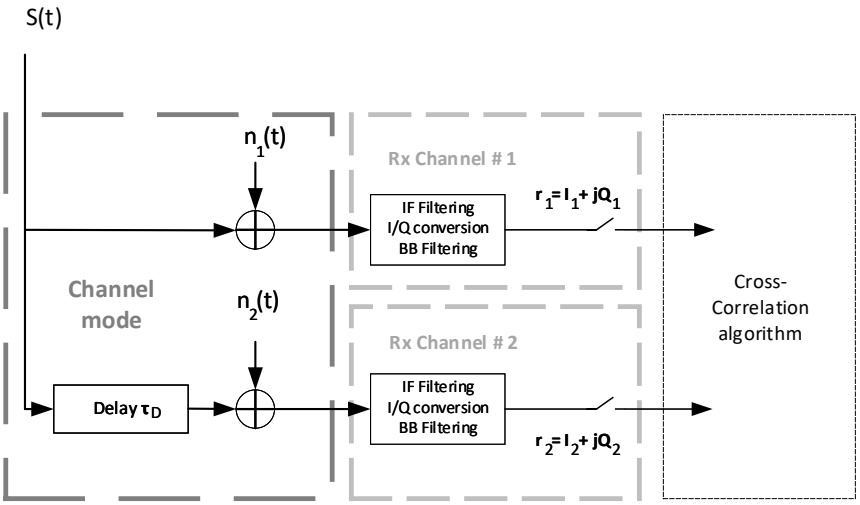

Figure 2.3: System model.

The cross-correlation points are acquired by averaging the product of the received signals. These values are then used to get the best fit of the parabolic curve. The maximum of this curve will be the time difference between the received signals as shown in Fig. 2.4. Fig. 2.5 shows the TDOA variance versus SNR for different types of transmitted signals.

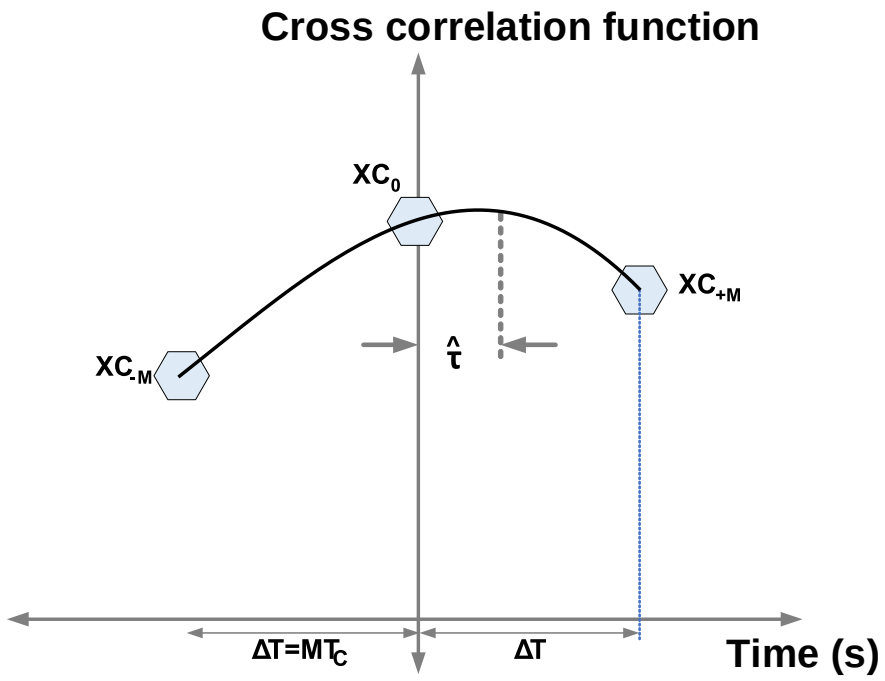

Figure 2.4: Interpolation of the cross-correlation values.

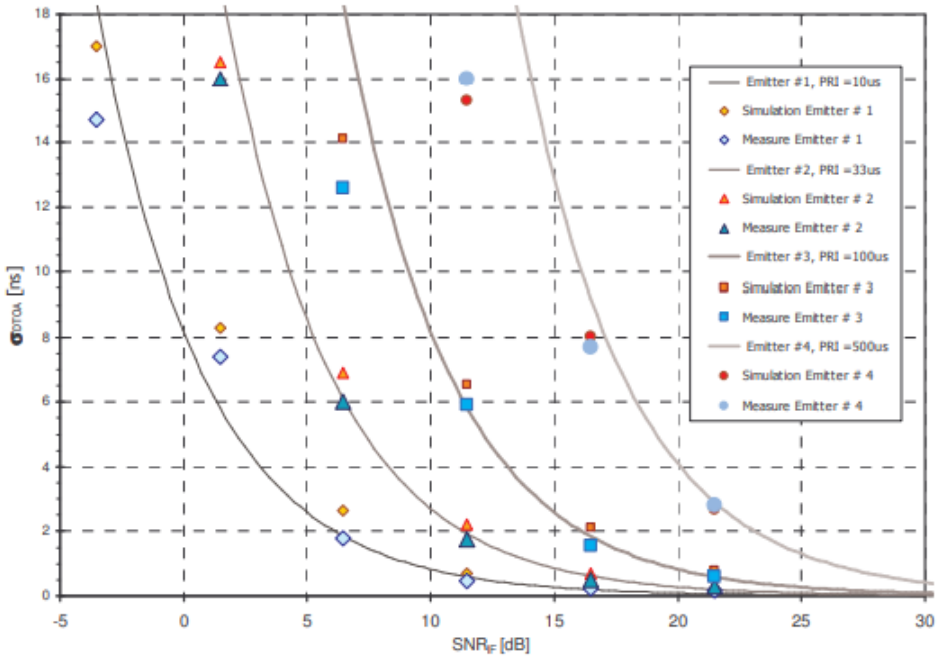

Figure 2.5: TDOA estimation: measured vs. expected results [24].

In [30], the authors found out that the two step approaches are sub-optimal and decided to use a single step approach; direct position maximum likelihood estimator whose results outperformed the two step approaches. This method can be applied to all types of signals−narrowband, wideband, lowpass or bandpass signals. This was studied for two cases. Case 1: when the transmitted signal is unknown and Case 2: when the transmitted signal is known but the transmission time is not. The example illustrated in Fig. 2.6 shows a transmitter placed at coordinates (135,75) Km, while the receivers are placed as in the figure on two lines perpendicular on one another. The transmitter

is assumed to be very far compared to the largest distance between the receivers:

$$T_{obs} > \frac{d_{\max}}{u}. \tag{2.8}$$

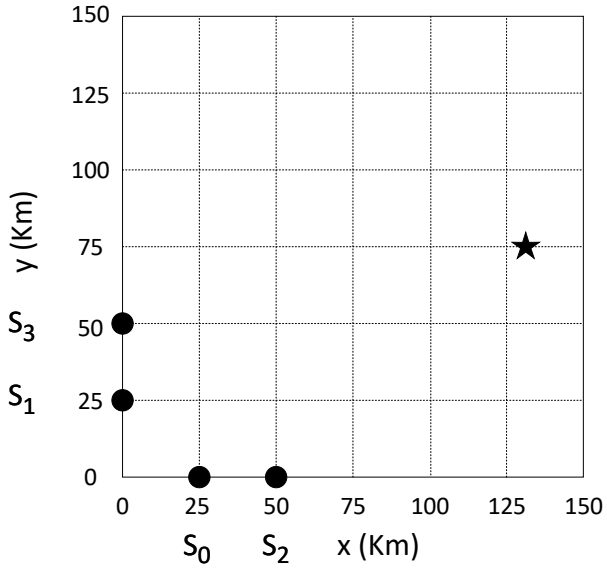

Figure 2.6: Structure of sensors (for $M = 4$) and transmitter position used in simulation.

For the first case when the transmitted signal was unknown, Fourier series was used to transform the signal to a form where they can have a parameter estimation. The transmitter coordinate is estimated as

$$(\hat{x}_t, \hat{y}_t) = \arg\ \lambda_{\max}(B'), \tag{2.9}$$

that is the maximum eigenvalue of

$$B' = Y'Y'^T = \sum_{i=0}^{M-1} (Y'Y'^T)$$

and

$$Y' = [\ y'_0\ y'_1\ ...\ y'_{M-1}\ ]$$

while

$$y'_0 = \int_0^T r_i(t)h(t-\tau_i)dt$$

such that $h(t)$ is the vector of sinusoids of the Fourier series and r_i is the ith received signal

$$h(t) = \left[\frac{1}{\sqrt{2}}\cos(2\pi F_0 t)\ ...\cos(2\pi(N-1)F_0 t)\sin(2\pi F_0 t)\ ...\sin(2\pi(N-1)F_0 t)\right]^T. \tag{2.10}$$

Although with this approach the matrices involved to obtain the ML estimate, the CRLB and and Fisher information matrix (FIM) are difficult to derive, this approach is adaptable to any signal type.

For the second case when the transmitted signal is known but the transmission time is not, no Fourier series was necessary. It was found that the estimate for the transmitter coordinates can be acquired by cross correlating the received and transmitted signals summed over all the sensors as represented in the below equation:

$$(x_t, y_t) = \arg\max \sum_{i=0}^{M-1} (\int_0^T r_i(t)S(t-\tau_i)dt)^2 \tag{2.11}$$

where M is the number of sensors, T is the observation interval, r_i is the ith received

signal and $S(t)$ is the transmitted signal.

In the simulations, the two-step method was implemented by first cross correlating each of the received signals with the received signal at the reference sensor to get the time difference of arrival. then an area of 1 Km $\times$ 1Km around the true transmitter position was split into 100×100 grids. The delay at each grid point was calculated using

$$\tau_i^{'} = \frac{\sqrt{(x_T - x_i)^2 + (y_t - y_i)^2}}{c} - \frac{\sqrt{(x_T - x_0)^2 + (y_t - y_0)^2}}{c}; i = 1, 2, ...M - 1, \quad (2.12)$$

and compared to the delay obtained from the cross correlation in the first step. Then, a squared error between the calculated value (using equation above) and the estimated value in the first step. The grid point that yielded the least square error was considered the estimated transmitter position.

$$LSE = \sum_{i=1}^{M-1} (\hat{\tau}_i^{'} - \tau_i^{'})^2 \quad (2.13)$$

where $\hat{\tau}_i^{'}$ is the TDOA estimated at the first step.

The direct positioning maximum likelihood estimator method was implemented for an area of 1Km $\times$ 1 Km, which is divided into 100×100 grids. This method is very complex but the results showed much better performance than the two-step algorithm as shown in Fig. 2.7.

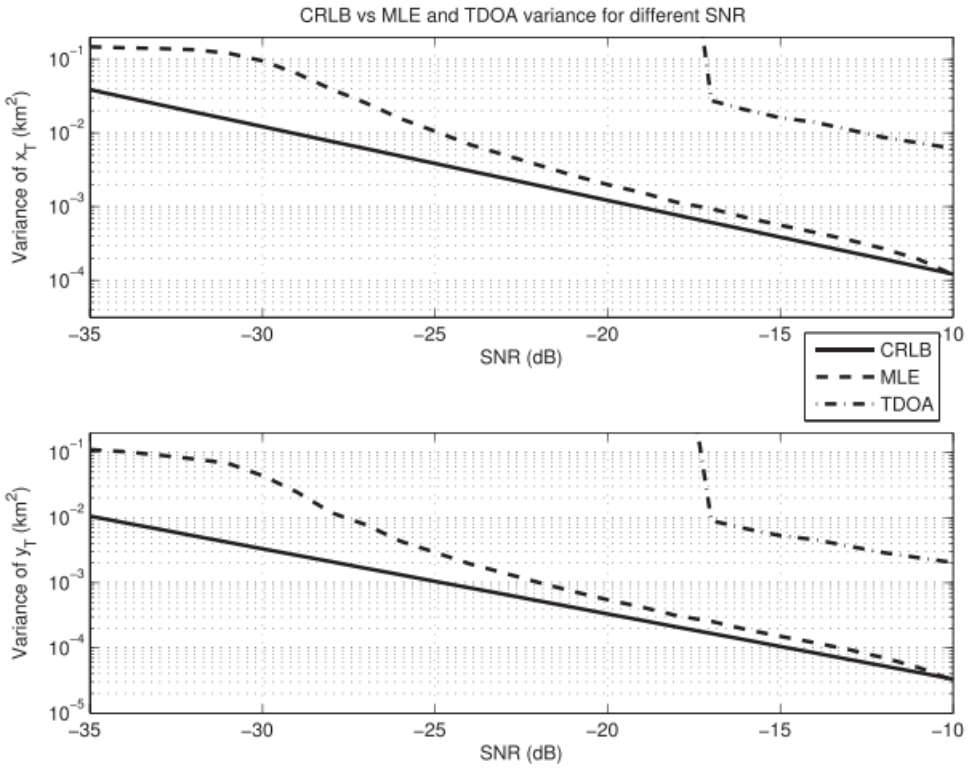

Figure 2.7: Comparison of MLE, TDOA and CRLB for different SNR values.

2.2 Angle of Arrival Estimation

In [12] and [27] the authors focused on one of the most widely used and efficient algorithms for AOA estimation: the Multiple Signal Classification (MUSIC) algorithm. MUSIC was studied extensively and its performance has been proved to be robust and adaptable to many signal types.

MUSIC is a peak search method for AOA estimation. It uses the the decomposition

of the eigenvalues of the co-variance matrix of the received signals. It can be applied in scenarios with single or multiple transmitters. A condition is that the number of receivers must be greater than the number transmitters. The general equation describing the MUSIC algorithm is

$$\begin{bmatrix} X_1 \\ X_2 \\ : \\ X_M \end{bmatrix} = \begin{bmatrix} a(\theta_1) & a(\theta_2) & .... & a(\theta_D) \end{bmatrix} \begin{bmatrix} F_1 \\ F_2 \\ : \\ F_D \end{bmatrix} + \begin{bmatrix} W_1 \\ W_2 \\ : \\ W_M \end{bmatrix} \tag{2.14}$$

where M is the number of receivers and D is the number of transmitters. This equation can be written in a compact matrix-vector form as

$$\boldsymbol{x} = \boldsymbol{A}\boldsymbol{f} + \boldsymbol{w}, \tag{2.15}$$

where matrix $\mathbf{A}$ is the steering vector with a dimension $M \times D$. It represents the phase shift between each received signal and the reference signal. As in [12] a single vector of the steering matrix can be written as

$$a(\theta_k) = \begin{bmatrix} 1 \\ e^{-j\frac{2\pi d_1 \sin(\theta_k)}{\lambda}} \\ : \\ e^{-j(D-1)\frac{2\pi d_{p-1} \sin(\theta_k)}{\lambda}} \end{bmatrix}. \tag{2.16}$$

The equation for the MUSIC algorithm is

$$\theta_{MUSIC} = \underset{min}{\arg} \; \beta^H(\theta) \; Q_N \; Q_N^H \; \beta(\theta) \tag{2.17}$$

where β is the signal sub-space and Q_N is the noise subspace, and they are orthogonal

to each other.

$$P_{MUSIC} = \frac{1}{\theta_{MUSIC}}. \tag{2.18}$$

In the simulations, the peaks of the P_{MUSIC} equation occurs when the AOA is equal to θ as illustrated in Fig. 2.8. The above equations are all valid when the signals are coherent. In [12] an improved MUSIC algorithm was proposed to work with non-coherent signals by adding an identity transition matrix $\mathbf{T}$ to the equation so that the new received signal matrix is defined as

$$\boldsymbol{x} = \boldsymbol{T}\boldsymbol{j}^* \tag{2.19}$$

where J^* denotes the complex conjugate of the original received signal.

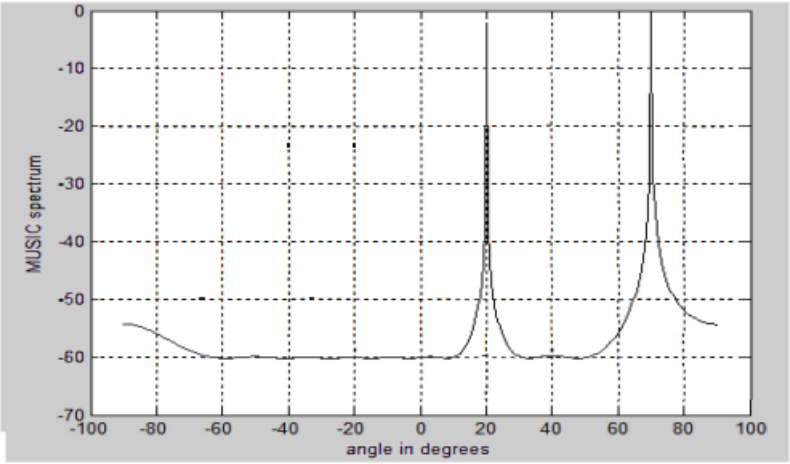

Figure 2.8: Spatial spectrum for MUSIC algorithm.

Existing work have used other algorithms to estimate the AOA such as a biased estimator as discussed in [28]. Also, one of the most commonly used algorithms used is the Estimation of Signal Parameters via Rotational Invariance Technique (ESPRIT)

which makes use of sub-arrays (named as doublets) within the main array to find the AOAs. But the MUSIC algorithm outperforms both. Many papers compared the performances of ESPRIT, MUSIC, and other algorithms (e.g., [25, 26]), MUSIC was shown to outperform both the above algorithms.

2.3 Hybrid TDOA/AOA Method

In [9] and [10], a hybrid TDOA/AOA solution was implemented to estimate the transmitter longitude and latitude. The transmitter was mobile and it was assumed to be moving at a far distance from the antennas so as to validate the assumption of having parallel incident signals. For TDOA, three fixed stations were placed in a triangular shape. The AOA used a single station of the three. The shared station was considered the central control server (CCS) at which the computation of the AOA bearing line and TDOA cross correlation algorithms were done. All the received signals at different stations are sent to the central control server for algorithms computation. The authors used the intersection of the hyperbolic curves from the TDOA along with the bearing line obtained from the AOA to estimate the transmitter location which was done also at the CCS.

Simulations showed that the range of coverage of the 3 receivers was approximately 20 $\sim$ 30Km. An advantage of this approach is that the range of detection can be increased by increasing the number of receivers at the expenses of an increased cost.

Chapter 3: Proposed Scheme

3.1 System Model

The architecture of the proposed system is shown in Fig. 3.1, which consists of a transmitter, whose position is to be estimated, the channel and one array of three receivers. Each receiver has a single antenna. A double sideband with carrier signal is used as input for the TDOA, where the carrier is only used as the signal for AOA. This is done to increase diversity and avoid redundant information. As shown in Fig. 3.1, the AOA input signal is a concatenation of the carrier and a sequence of zeros. This concatenation is needed because the modified AOA method implemented in this work does not restrict the phase difference between the received signals to a fraction of the period (i.e., a maximum of 2π phase difference) as the spacing between antennas can be multiples of λ.

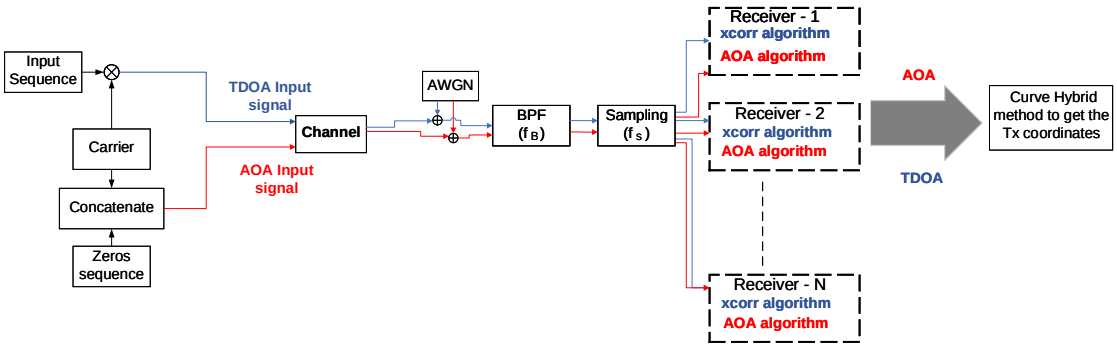

Figure 3.1: System block diagram.

A maximum likelihood estimator is used to estimate the time difference between the received signals. This will be explained in detail in Section 3.2. Another maximum likelihood estimator is used to estimate the angles of arrival at each receiver, which will be explained in detail in Section 3.3. The last block combines the outputs of the TDOA and AOA blocks to estimate the transmitter coordinates. The transmitted signals are filtered at the receiver as described in [13] before sampling to limit the additive white Gaussian nose (AWGN) bandwidth so as to limit its power. The noise samples are therefore band-limited.

The arrangement of transmitter and receivers is illustrated in Fig. 3.2, for a simple case of 2D positioning with one array of receivers (here 3 as a example) placed equidistantly and collinearly, and a single transmitter.

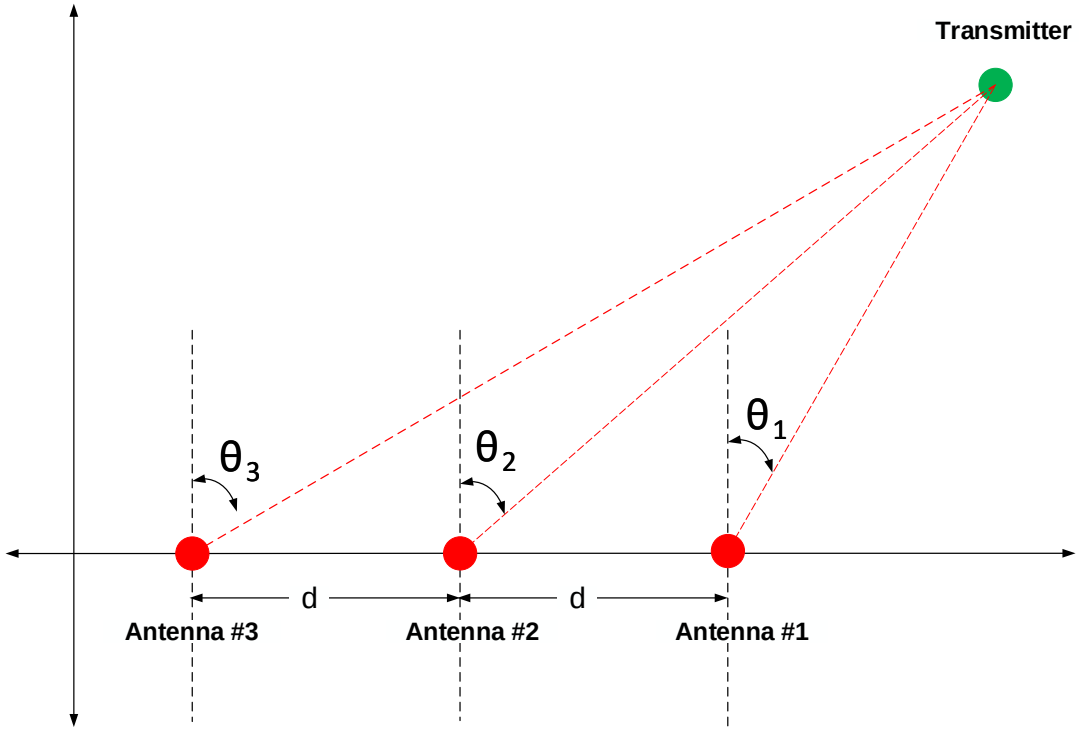

Figure 3.2: Transmitter and receivers arrangement.

3.2 TDOA Approach

In TDOA systems the received signals are expressed as

$$\mathbf{r} = \mathbf{s}(\boldsymbol{\tau}) + \mathbf{e} \tag{3.1}$$

$$\mathbf{r} = \begin{bmatrix} r1 \\ r2 \\ r3 \end{bmatrix} = \begin{bmatrix} as(t-\tau_1) \\ as(t-\tau_2) \\ as(t-\tau_3) \end{bmatrix} + \begin{bmatrix} e_1 \\ e_2 \\ e_3 \end{bmatrix} \tag{3.2}$$

where τ_1, τ_2 and τ_3 are the differences in time compared to the the time when the signal was transmitted initially. The absolute initial transmission time is assumed to be unknown in TDOA systems; thus, τ_1 can be used as the reference time (i.e., assuming it equals zero). Accordingly, all the time delays will be calculated with respect to receiver 1 and thus named as τ_{12} and τ_{13} and the above vector equation can be rewritten as

$$\mathbf{r} = \begin{bmatrix} r1 \\ r2 \\ r3 \end{bmatrix} = \begin{bmatrix} as(t-\tau_{11}) \\ as(t-\tau_{12}) \\ as(t-\tau_{13}) \end{bmatrix} + \begin{bmatrix} e_1 \\ e_2 \\ e_3 \end{bmatrix} \tag{3.3}$$

where τ_{11} is equal to zero. We exploit the maximum Likelihood estimator to estimate the transmitter position using the TDOAs. The vector of the parameters required to be estimated $\boldsymbol{\tau}$ can be defined as

$$\boldsymbol{\tau} = \begin{bmatrix} \tau_{12} \\ \tau_{13}. \end{bmatrix} \tag{3.4}$$

The error is assumed to have a normal distribution of zero mean and variance equals σ^2. Thus, the probability density function of r_1 is $p_{r_1}(r_1)$ is defined as

$$p_{r_1}(r_1) = \frac{1}{\sqrt{2\pi\sigma^2}} e^{\frac{-(r_1 - s(t-\tau_{11}))^2}{2\sigma^2}} \tag{3.5}$$

Accordingly, the conditional probability can be expressed as

$$p_{r_1}(r_1|\tau) = \frac{1}{\sqrt{2\pi\sigma^2}} e^{\frac{-(r_1 - as(t-\tau_{11}))^2}{2\sigma^2}} \tag{3.6}$$

Since the observations are independent, the PDF of the observation vector $\mathbf{r}$ can be

written as

$$\begin{aligned} p_{\mathbf{r}}(\mathbf{r}|\boldsymbol{\tau}) &= \prod_{i=1}^{N} p_{r_i}(r_i|\boldsymbol{\tau}) \\ &= \frac{1}{(2\pi\sigma^2)^{\frac{N}{2}}} e^{\frac{-\sum_{i=1}^{N}(r_i - as(t-\tau_{1i})^2}{2\sigma^2}}, N = 3 \end{aligned} \tag{3.7}$$

In order to get the ML estimator, taking the logarithm of the above equation results in

$$\mathbf{L}_{TDOA} = \log\ p_r(r_1\ r_2\ r_3|\ \boldsymbol{\tau}) = -\frac{N}{2}\log\ (2\pi\sigma^2) - \frac{\sum_{i=1}^{N}(r_i - as(t-\tau_{1i}))^2}{2\sigma^2}. \tag{3.8}$$

To obtain the transmitter coordinators using only TDOAs, we resort to the following equations for calculating τ_{12} and τ_{13}:

$$\tau_{12} = \frac{1}{c}\ \times (\sqrt{(x_1 - x_t)^2 + (y_1 - y_t)^2}\ -\ \sqrt{(x_2 - x_t)^2 + (y_2 - y_t)^2}). \tag{3.9}$$

$$\tau_{13} = \frac{1}{c}\ \times (\sqrt{(x_1 - x_t)^2 + (y_1 - y_t)^2}\ -\ \sqrt{(x_3 - x_t)^2 + (y_3 - y_t)^2}). \tag{3.10}$$

The corresponding values of x_t and y_t that will yield the maximum value of the logarithmic expression will be the transmitter coordinates.

$$\hat{\tau} = arg_{\tau}\ max\ \mathbf{L}_{TDOA} \tag{3.11}$$

3.3 AOA Approach

A condition differing from previous work for the AOA approach considered here is that the system operates in 'near field', meaning that the distance between the transmitter and the array of receiving antennas is not significantly larger than the antenna spacing to allow all receivers to have the same AOA. Besides, the spacing between the array

antennas is not restricted to a maximum of half the signal wavelength as in past work. It can be multiples of the signal wavelength. As a result, each receiver has a different angle of arrival and the incident waves can not be assumed to be parallel anymore.

The difference in distance traveled by the signal between each receiver and the reference one is illustrated in Fig. 3.3.

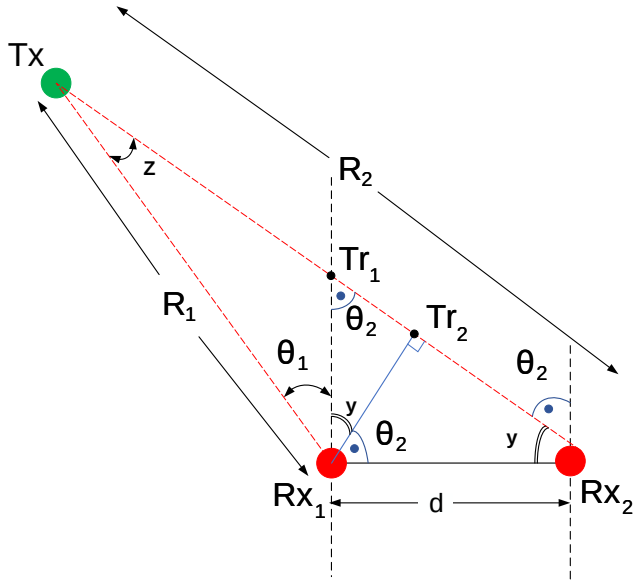

Figure 3.3: Rx_1 and Rx_2.

$$Tr_2\ Rx_2\ = d \sin\theta_2 \tag{3.12}$$

$$Rx_1\ Tr_2\ = d \cos\theta_2 \tag{3.13}$$

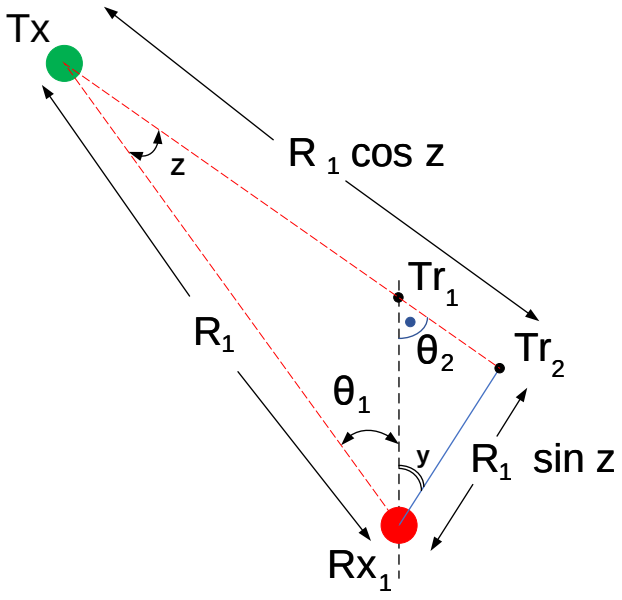

Figure 3.4: Distance travelled to Rx_1.

Fig. 3.4 shows the triangle $Tx\ Tr_2\ Rx_1$. The following equations apply to get R_1 which is the distance travelled by the signal from the transmitter Tx to receiver 1 (Rx_1):

$$\begin{aligned} d\cos\theta_2 &= R\sin Z \\ &= R_1\sin(90^\circ - \theta_1 - y) \\ &= R_1\cos(-\theta_1 - y) \\ &= R_1\cos(-\theta 1 + \theta_2 - 90^\circ \\ &= R_1\sin(\theta_2 - \theta 1) \\ \implies R_1 &= d\,\frac{\cos\theta_2}{\sin(\theta_2 - \theta_1)} \end{aligned} \tag{3.14}$$

The expression for the distance from Tx to Rx_2 can be derived as the following

$$\begin{aligned}
R_2 &= d\sin\theta_2 \ + \ R_1\cos Z \\
&= d\sin\theta_2 + \frac{d\cos\theta_2}{\sin(\theta_2-\theta_1)}\cos z \\
&= d\sin\theta_2 \ + \frac{d\cos\theta_2}{\sin(\theta_2-\theta_1)}\cos(90^\circ-\theta_1-y) \\
&= d\sin\theta_2 \ + \frac{d\cos\theta_2}{\sin(\theta_2-\theta_1)}\cos(-(\theta_1+y-90^\circ)) \\
&= d\sin\theta_2 \ + \frac{d\cos\theta_2}{\sin(\theta_2-\theta_1)}\cos(\theta_1+y-90^\circ) \\
&= d\sin\theta_2 \ + \frac{d\cos\theta_2}{\sin(\theta_2-\theta_1)}\sin(\theta_1+y) \\
&= d\sin\theta_2 \ + \frac{d\cos\theta_2}{\sin(\theta_2-\theta_1)}\sin(\theta_1+90^\circ-\theta_2) \\
&= d\sin\theta_2 \ + \frac{d\cos\theta_2}{\sin(\theta_2-\theta_1)}\cos(\theta_1-\theta_2)
\end{aligned} \tag{3.15}$$

The difference in distances travelled between R_1 and R_2 can be expressed as

$$\begin{aligned}
\Delta d \ &= R_1 - R_2 \\
&= d\ \frac{\cos\theta_2}{\sin(\theta_2-\theta_1)} \ - \ d\sin\theta_2 \ - \ d\ \frac{\cos\theta_2}{\sin(\theta_2-\theta_1)}\cos(\theta_1-\theta_2) \\
\implies \Delta d \ &= d\ [\frac{\cos\theta_2\ (1-\cos(\theta_1-\theta_2))}{\sin(\theta_2-\theta_1)} - \sin\theta_2].
\end{aligned} \tag{3.16}$$

Using the above expressions to get the phase difference between the received signals at each receiver and the reference receiver Rx_1 using the relationship below:

$$\begin{aligned}
\Delta\phi \ &= \ 2\pi f\Delta\tau \\
&= \ 2\pi f\frac{\Delta d}{u} \\
&= \ \frac{2\pi}{\lambda}\Delta d
\end{aligned} \tag{3.17}$$

Thus, the received signals at each receiver can be written in the following vector form

$$\mathbf{g} = \mathbf{h}(\theta) + \mathbf{w}. \tag{3.18}$$

For the example with three receivers,

$$\mathbf{g} = \begin{bmatrix} g_1 \\ g_2 \\ g_3 \end{bmatrix} = \begin{bmatrix} 1 \\ a(\theta_1, \theta_2) \\ a(\theta_1, \theta_3) \end{bmatrix} \begin{bmatrix} F_1 \end{bmatrix} + \begin{bmatrix} w_1 \\ w_2 \\ w_3 \end{bmatrix} \tag{3.19}$$

where F_1 is the transmitted signal. The AOAs that need to be estimated, i.e., vector $\boldsymbol{\theta}$, is written as

$$\boldsymbol{\theta} = \begin{bmatrix} \theta_1 \\ \theta_2 \\ \theta_3 \end{bmatrix} \tag{3.20}$$

and $a(\theta_1, \theta_2)$ is the phase difference between the received signals at g_1 and g_2 and $a(\theta_1, \theta_3)$ is the phase difference between the received signals at g_1 and g_3 expressed as

$$a(\theta_1, \theta_2) = e^{j\frac{2\pi}{\lambda} d \left[\frac{\cos\theta_2}{\sin(\theta_2 - \theta_1)} \ (1 - \cos(\theta_2 - \theta_1)) - \sin\theta_2\right]} \tag{3.21}$$

$$a(\theta_1, \theta_3) = e^{j\frac{2\pi}{\lambda} 2 \ d \left[\frac{\cos\theta_3}{\sin(\theta_3 - \theta_1)} \ (1 - \cos(\theta_3 - \theta_1)) - \sin\theta_3\right]} \tag{3.22}$$

Since the first element of steering vector, a_1, equals one, it carries no information about θ_1, which mandates having more than one reference receiver to be able to get the corresponding AOA at each receiver. Accordingly, vector the g will be updated as:

$$\mathbf{g} = \begin{bmatrix} g_2 \\ g_3 \\ g_{23} \end{bmatrix} = \begin{bmatrix} a(\theta_1, \theta_2) \\ a(\theta_1, \theta_3) \\ a(\theta_2, \theta_3) \end{bmatrix} \begin{bmatrix} F_1 \end{bmatrix} + \begin{bmatrix} w_2 \\ w_3 \\ w_3 \end{bmatrix}. \tag{3.23}$$

Receiver 2 was used as a reference too to add $a(\theta_2, \theta 3)$ in the steering vector. g_{23} is the

received signal at antenna 3 with a phase difference calculated with respect to receiver 2 as

$$a(\theta_2, \theta_3) = e^{j\frac{2\pi}{\lambda}d\ [\frac{\cos\theta_3}{\sin(\theta_3-\theta_2)}\ (1-\cos(\theta_3-\theta_2))-\sin\theta_3]}. \tag{3.24}$$

The maximum likelihood estimator can be used for the above vector equation. The observation vector g is the received vector. The steering vector multiplied by the transmitted signal F_1 equals $h(\theta)$. Just like the case in TDOA, the error has a normal distribution of zero mean and variance which equals σ^2. Then, the PDF of g_1 is $p_{g_1}(g_1)$, which have the same distribution with a shifted mean and can be written as

$$p_{g_1}(g_1) = \frac{1}{\sqrt{2\pi\sigma^2}} e^{\frac{-(g_1-h_1)^2}{2\sigma^2}}. \tag{3.25}$$

Similarly, the conditional probability can be expressed as

$$p_{g_1}(g_1|\theta) = \frac{1}{\sqrt{2\pi\sigma^2}} e^{\frac{-(g_1-h_1)^2}{2\sigma^2}}. \tag{3.26}$$

Since, the observations are independent, the PDF of the observation vector g can be written as

$$\begin{aligned} p_{\mathbf{g}}(\mathbf{g}|\boldsymbol{\theta}) &= \prod_{i=1}^{N} p_{g_i}(g_i|\boldsymbol{\theta}) \\ &= \frac{1}{(2\pi\sigma^2)^{\frac{N}{2}}} e^{\frac{-\sum_{i=1}^{N}(g_i-h_i(\theta))^2}{2\sigma^2}}, N = 3. \end{aligned} \tag{3.27}$$

For the ML estimator, the logarithm of the previous equation is expressed as

$$\mathbf{L}_{AOA} = \log\ p_g(g_1\ g_2\ g_3|\ \theta) = -\frac{N}{2}\log\ (2\pi\sigma^2) - \frac{\sum_{i=1}^{N}(g_i - h_i(\theta))^2}{2\sigma^2}. \tag{3.28}$$

The angles of arrival that yield the maximum of the log-likelihood equation above correspond to the transmitter coordinate.

$$\hat{\theta} = arg_{\theta}\ max\ \mathbf{L}_{AOA} \tag{3.29}$$

3.4 TDOA and AOA Hybrid Solution

The AOA approach will yield the angles of arrival at each receiver while the TDOA approach will yield the time delays. These two pieces of information can be exploited together to to yield points that are closer to the transmitter $P13$ and $P12$ as shown in Fig. 3.5. With antenna 1 being the reference, $P13$ and $P12$ along with antenna 1 lies on an arc whose center would be the transmitter in the ideal case. The three are equidistant from the transmitter as shown in Fig. 3.5.

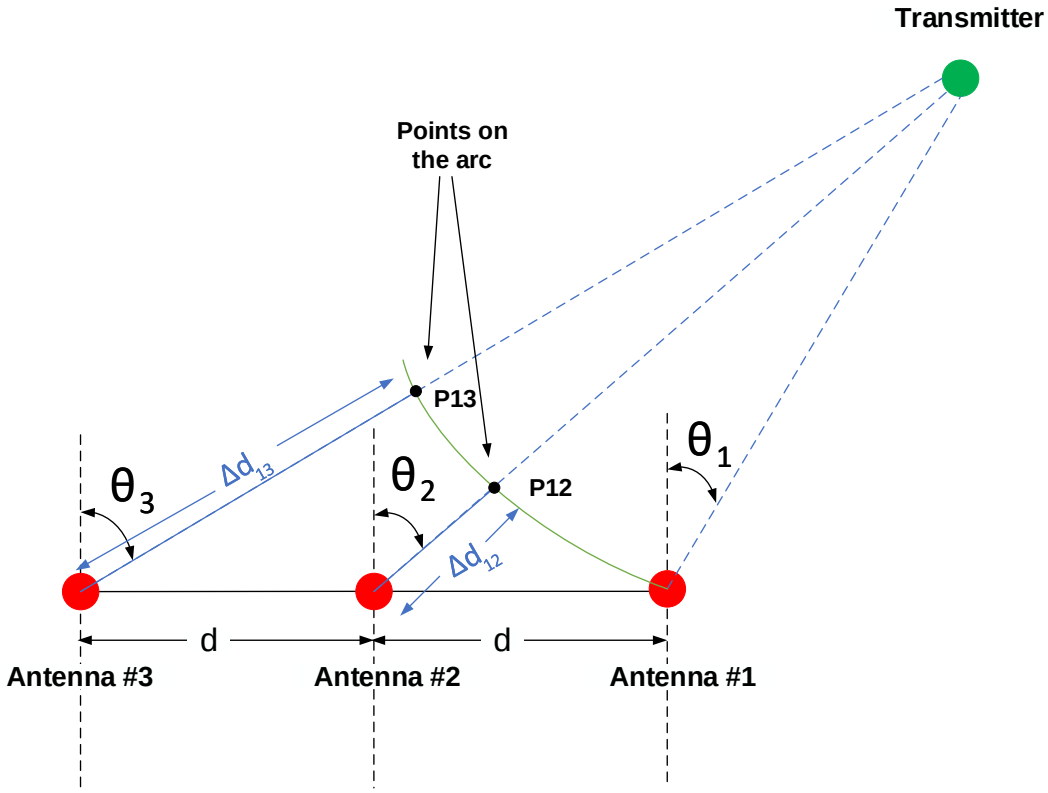

Figure 3.5: Illustration of the hybrid approach.

The coordinates of $P13$ and $P12$ are calculated by using the estimated AOAs and the TDOAs as in the following equations: x-coordinate of $P12$:

$$P12_x = Antenna\ 2\ _x + \mid \Delta d_{12} \mid \sin\theta_2. \tag{3.30}$$

y-coordinate of $P12$:

$$P12_y = Antenna\ 2\ _y + \mid \Delta d_{12} \mid \cos\theta_2. \tag{3.31}$$

x-coordinate of $P13$:

$$P13_x = Antenna\ 3\ _x + \mid \Delta d_{13} \mid \sin\theta_3. \tag{3.32}$$

y-coordinate of $P13$:

$$P13_y = Antenna\ 3\ _y + \mid \Delta d_{13} \mid \cos\theta_3. \tag{3.33}$$

The point at which the 3 distances to it are almost the same or have the least difference between one another is the transmitter coordinates. In other words the point that results in the minimum of of the following equation will be the estimated transmitter location:

$$f = \mid d_{1t} - d_{2t} \mid + \mid d_{1t} - d_{3t} \mid + \mid d_{2t} - d_{3t} \mid . \tag{3.34}$$

$$\hat{x_{grid}}, \hat{y_{grid}} = arg_{x,y}\ min\ \mathbf{f} \tag{3.35}$$

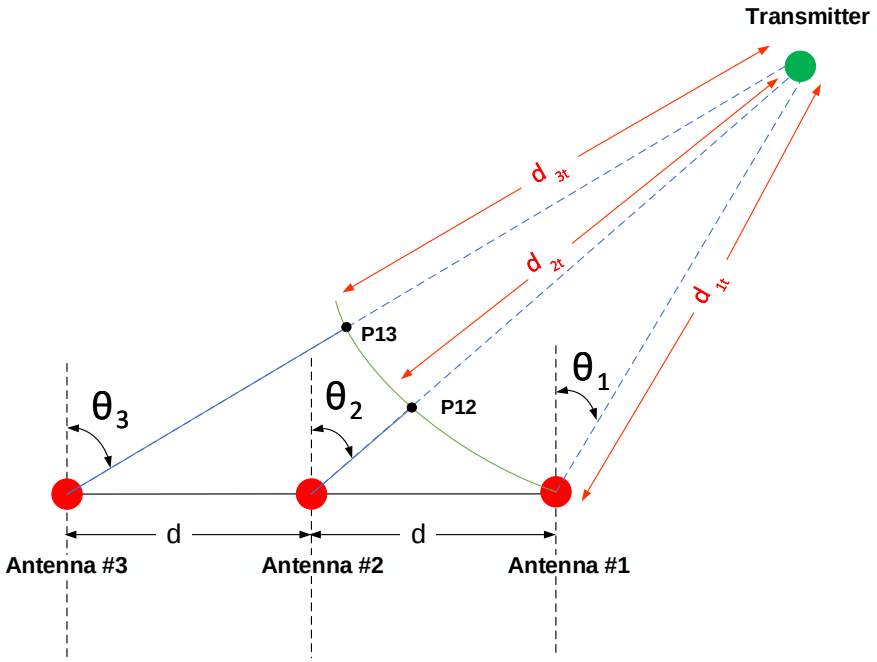

Figure 3.6: Equal radii arc

Chapter 4: Simulation Results

This chapter presents simulation results of the three implemented approaches. The TDOA approach, AOA approach and the hybrid approach. It also includes the system parameters and assumptions.

4.1 System Related Assumptions

The implemented 2D system is assumed to have three collinear antennas with a spacing d=3 m between each two adjacent antennas. The coordinates of the receivers and the transmitter are placed as shown in Fig. 4.1. The coverage area of this 2D system is a 180° plane; that is, the transmitted is assumed to be on half of the plane (the transmitter y-axis is non-negative).

The initial transmission time is assumed to be unknown but the input signal is assumed to be known at the receivers.

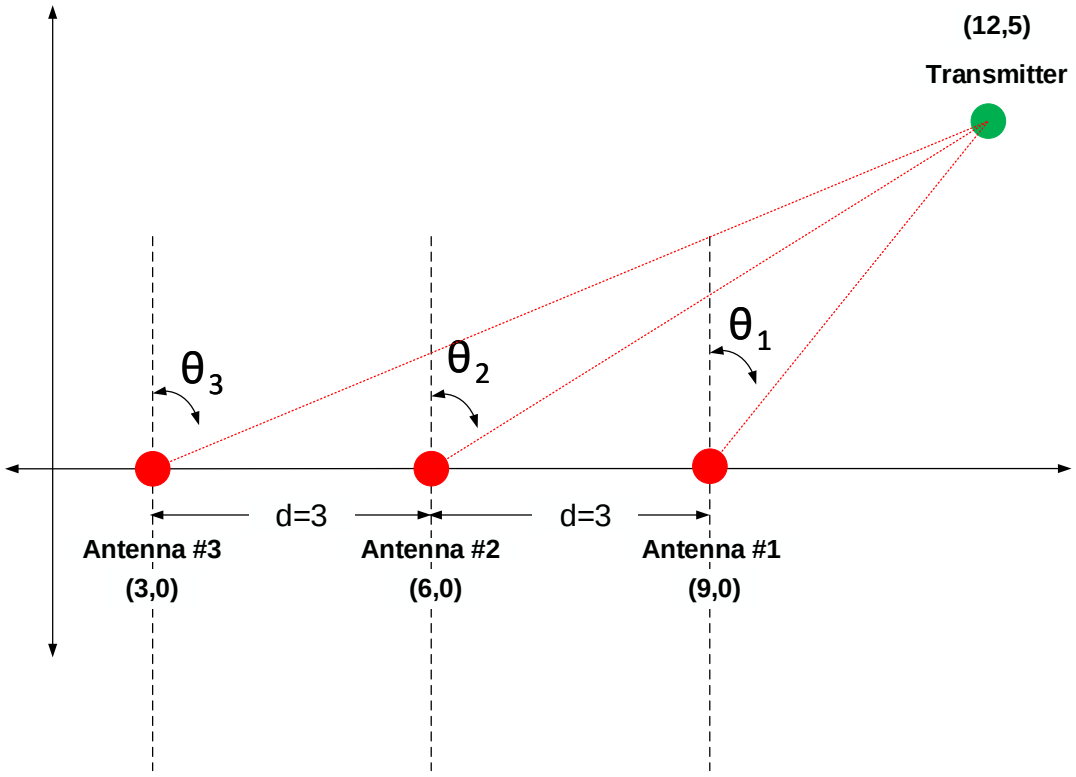

Figure 4.1: System coordinates.

4.2 Channel Assumptions

An ideal channel is assumed where the signal propagates via only a line-of-sight path with attenuation; that is, multipath fading effects are not considered. Additive white gaussian noise (AWGN) with zero mean and a standard deviation of $\sigma = 0.02$ is added to the signal.

4.3 TDOA Approach

The TDOA Approach baseband signal is assumed to be a sequence of ones and negative ones $\mathbf{in}_{TDOA_{seq}}$ as shown in Fig. 4.2. The input signal to the TDOA block is a double sideband with carrier that is represented by equation (4.1) for which an example is shown in Fig. 4.3.

$$\mathbf{v}_{TDOA_{in}} = A\cos(2\ \pi\ f_c\ t)\ \mathbf{in}_{TDOA_{seq}} \tag{4.1}$$

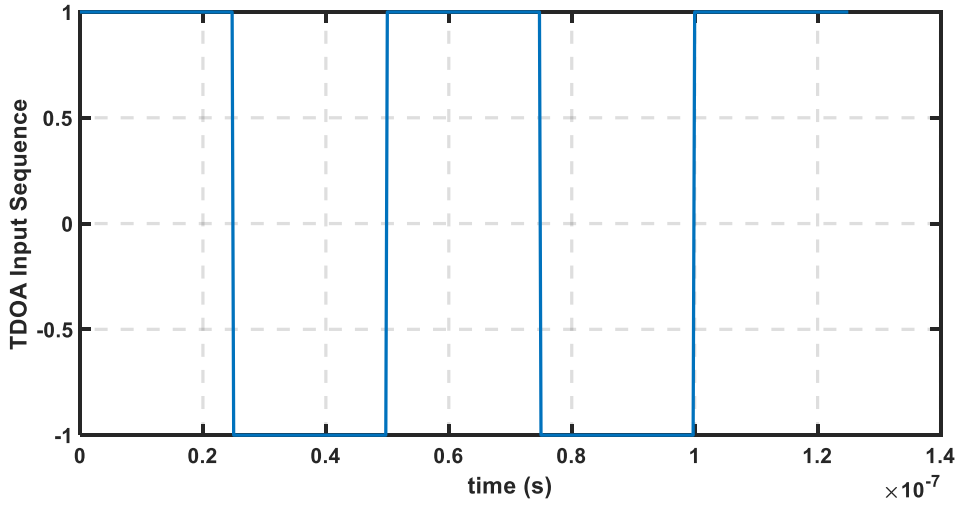

Figure 4.2: TDOA Approach baseband signal.

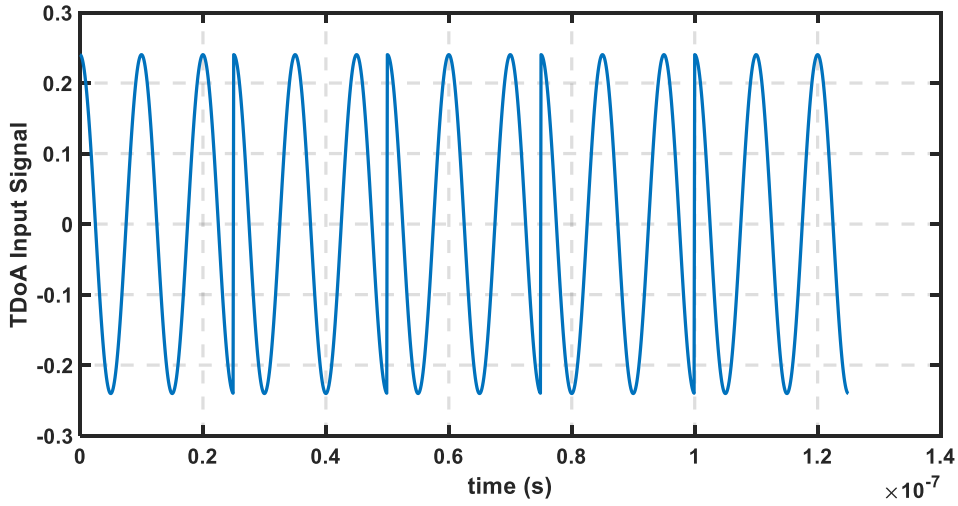

Figure 4.3: TDOA Approach input signal at SNR=5.3.

The received signals by each of the three receivers at SNR=5.3 are shown in Fig. 4.4, Fig. 4.5 and Fig. 4.6, respectively.

$$SNR = \frac{A_{Rx}}{\sigma} \tag{4.2}$$

A_{Rx} is the amplitude of the received signal.

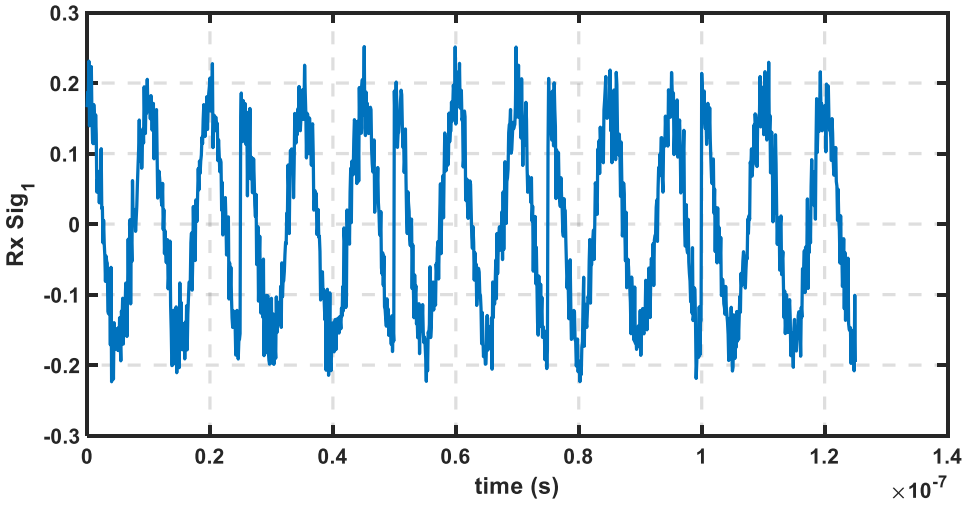

Figure 4.4: Signal received at Rx_1 *at* $SNR = 5.3$.

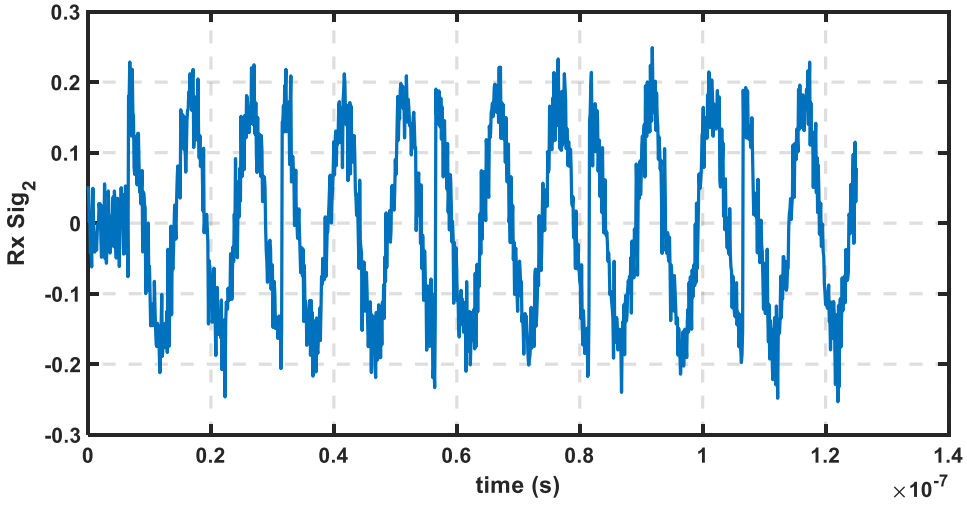

Figure 4.5: Signal received at Rx_2 *at* $SNR = 5.3$.

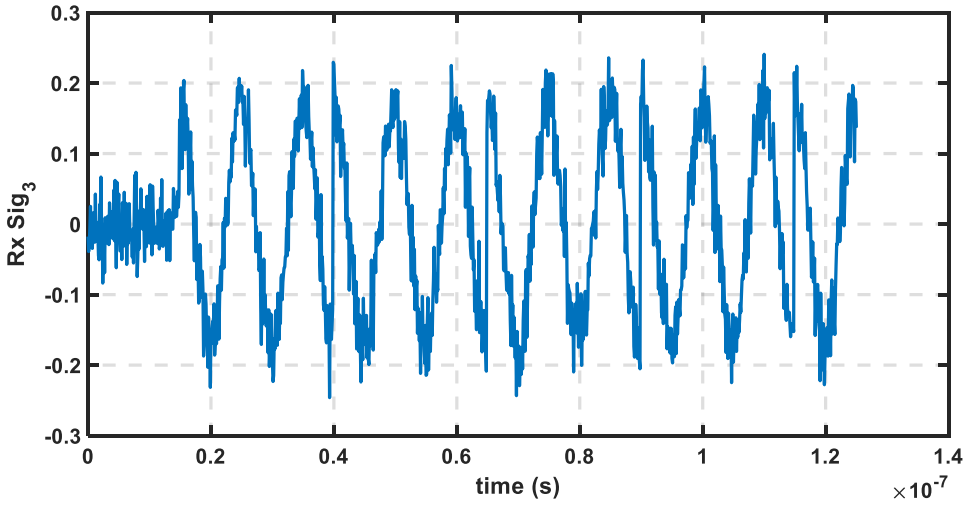

Figure 4.6: Signal received at Rx_3 *at* $SNR = 5.3$.

The TDOA approach is implemented as a two-step algorithm. First, an area of 50m×50m around the true transmitter position is divided into 100×100 grid points as shown in Fig. 4.7. For each grid, point, the TDOAs were calculated using:

$$\tau_{12} = \frac{1}{u} \times (\sqrt{(x_1 - x_{grid})^2 + (y_1 - y_{grid})^2} - \sqrt{(x_2 - x_{grid})^2 + (y_2 - y_{grid})^2}). \quad (4.3)$$

$$\tau_{13} = \frac{1}{u} \times (\sqrt{(x_1 - x_{grid})^2 + (y_1 - y_{grid})^2} - \sqrt{(x_3 - x_{grid})^2 + (y_3 - y_{grid})^2}). \quad (4.4)$$

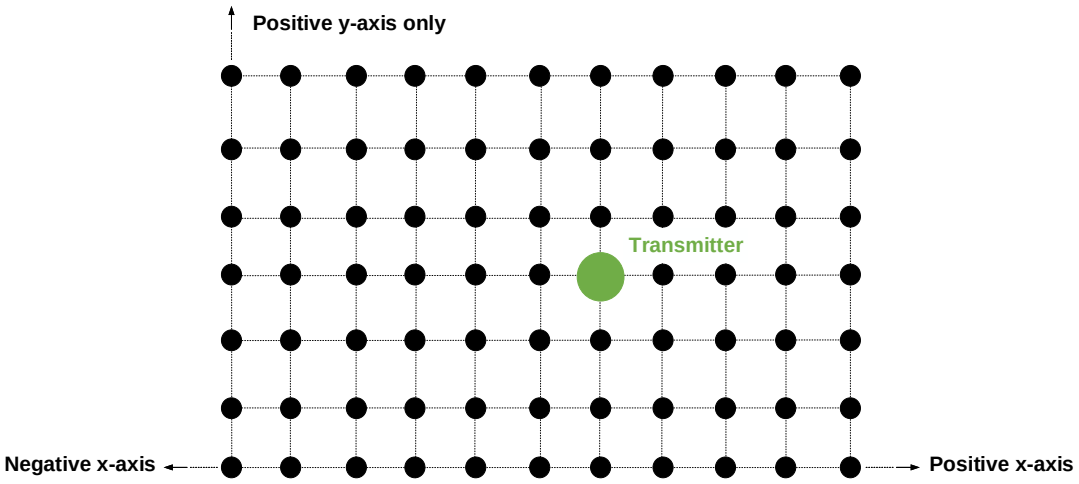

Figure 4.7: Sweeping area grid.

Since, the transmitted signal is known at the receiver side. These TDOAs are used to generate time shifted versions of the pre-determined input sequence for each receiver. Those time shifted signals and received signals are used to substitute in the log-likelihood equation $\mathbf{L}_{TDOA}$.

$$\mathbf{L}_{TDOA} = -\frac{3}{2}\log\,(2\pi\sigma^2) - \frac{\sum_{i=1}^{3}(r_i - as(t-\tau_{1i})_{grid})^2}{2\sigma^2}. \tag{4.5}$$

The grid point that yielded the maximum $\mathbf{L}_{TDOA}$ is the estimated transmitter position. The results are obtained from 500 Monte carlo simulations.

Figs. 4.8 and 4.9 show the estimated transmitted coordinates at SNR=5.3.

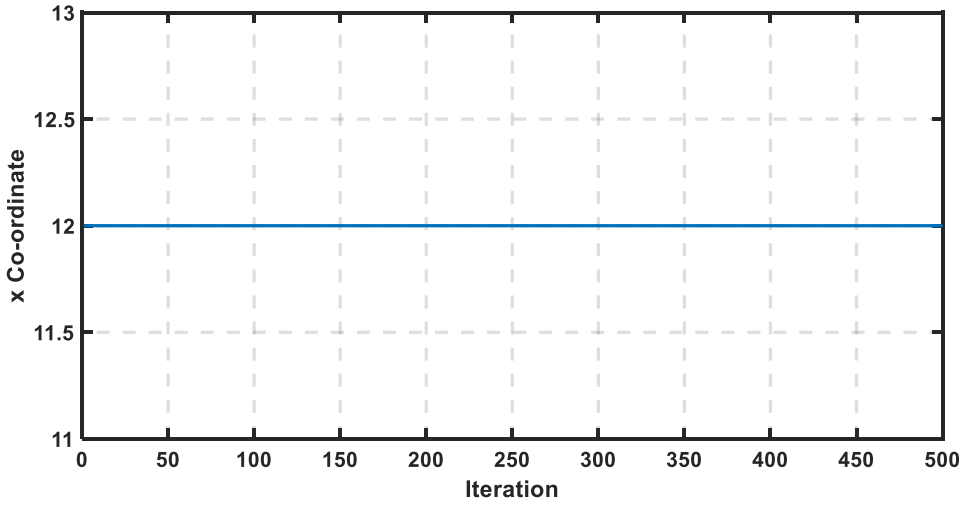

Figure 4.8: Estimated transmitter x-coordinate vs. iterations at SNR=5.3.

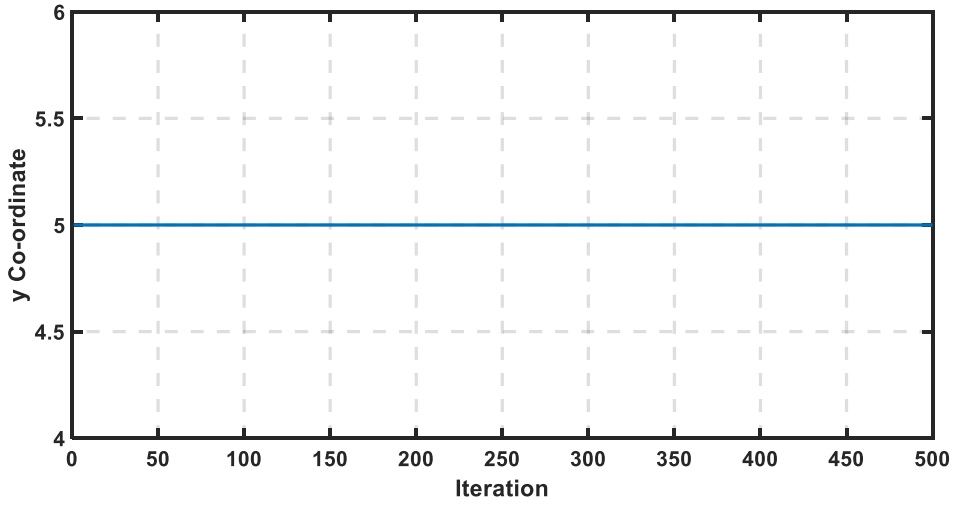

Figure 4.9: Estimated transmitter y-coordinate vs. iterations at SNR=5.3.

The MSE versus SNR curves for both x- and y-coordinates are shown in Fig. 4.10

and Fig. 4.11.

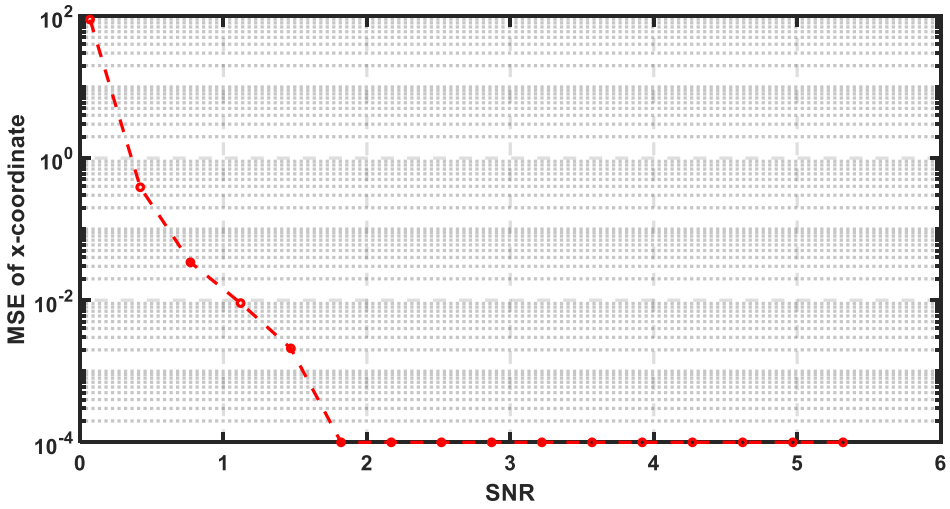

Figure 4.10: TDOA approach: MSE vs. SNR for x-coordinate.

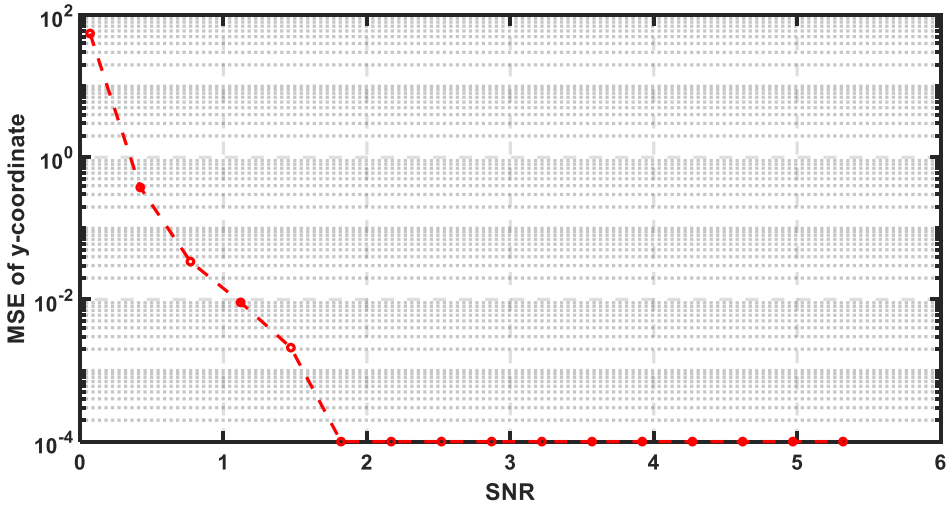

Figure 4.11: TDOA approach: MSE vs. SNR for y-coordinate.

If a whole 360° plane is to be covered, i.e., the negative part of the y-axis is included, then $\mathbf{L}_{TDOA}$ will have two equal maximum points. The corresponding x- and y-coordinates at these two points are the transmitter estimated locations as shown in Fig. 4.12. One of them is the true position and the other is its mirrored location on the x-axis as the TDOA depends on the absolute time difference only, and thus the two locations will yield the same maximum for $\mathbf{L}_{TDOA}$. Because the transmitter is restricted to be on the positive part of the y-axis only, this ambiguity does not exist in this research results.

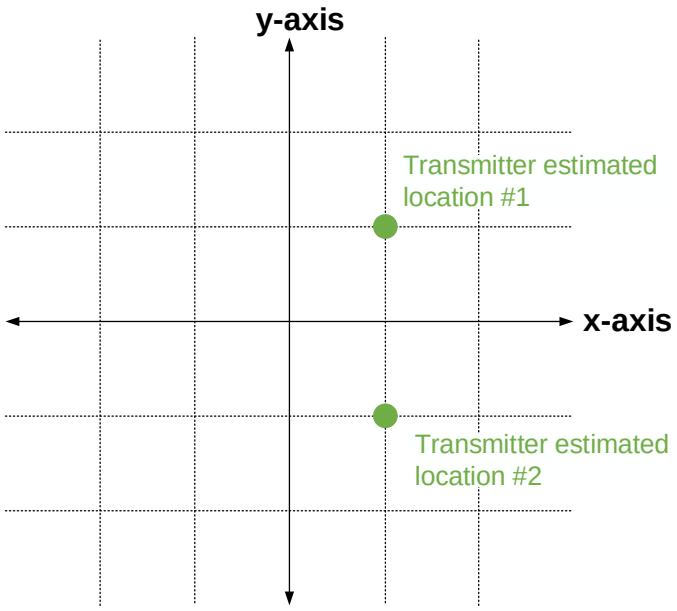

Figure 4.12: Estimated transmitter coordinates with a 360° sweep.

In prior work, TDOA approach showed better MSE than AOA approach in short ranges (i.e. when transmitter true position is close to the receiving antennas array) whilst

in longer ranges AOA approach showed better MSE results than TDOA approach. In Figs. 4.13 and 4.14, the transmitter was located at different distances from the receivers array.

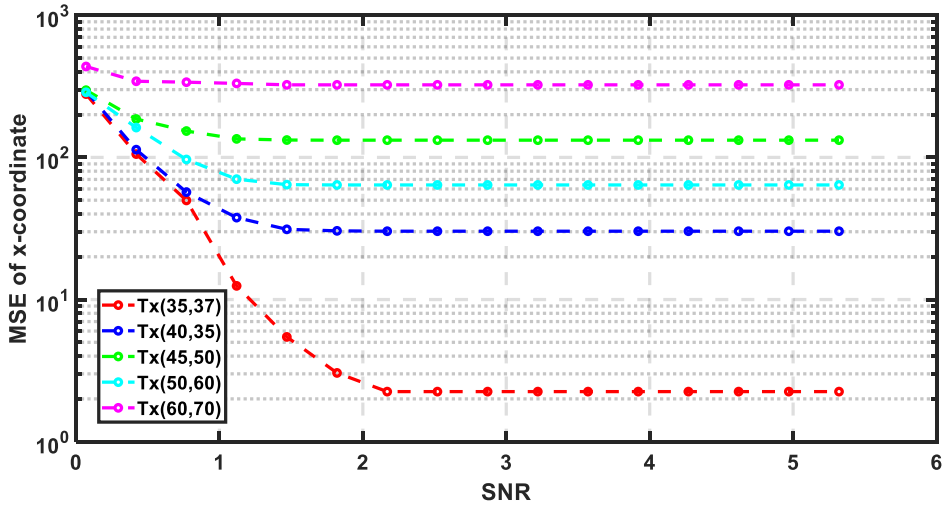

Figure 4.13: TDOA approach range − x-coordinate.

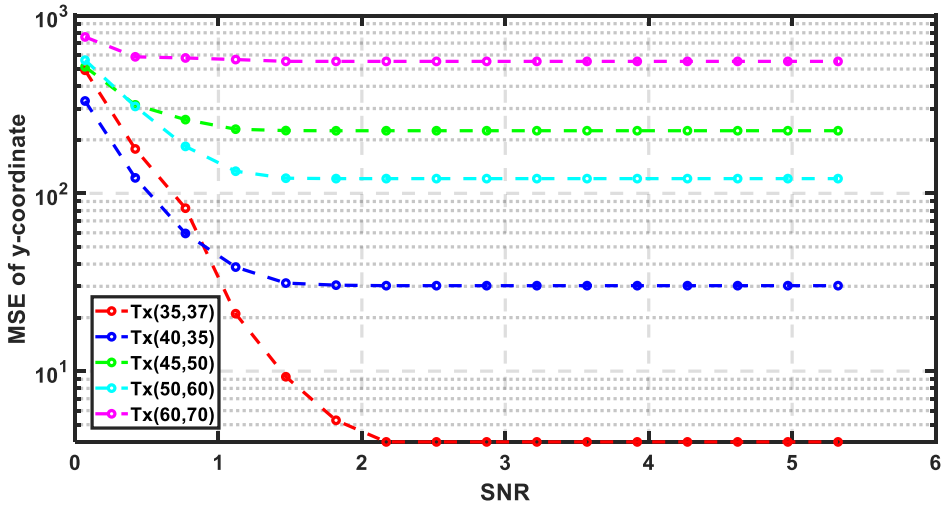

Figure 4.14: TDOA approach range – y-coordinate.

It is obvious from Figs. 4.13 and 4.14 that TDOA has quite a small range. It yielded the least MSE when the transmitter was located at (35,37). As the transmitter is moved further, its MSE leveled off at higher MSE values showing non robust results.

4.4 AOA Approach

The input signal for the AOA block is the carrier signal concatenated with a sequence of zeros expressed as

$$\mathbf{v}_{AOA_{in}} = A\cos(2\ \pi\ f_c\ t)\ \mathbf{in}_{AOA_{seq}}. \tag{4.6}$$

An example is shown in Fig. 4.15. Concatenation of a carrier with a period when no signal is transmitted means that $\mathbf{in}_{AOA_{seq}}$ is a sequence of ones and zeros. Selection of this special input signal is to make sure that the periodicity of the carrier signal does

not cause any problems in detecting the phase difference between the received signals, since in this modified AOA algorithm, the spacing between the antennas is not restricted to a maximum of one wavelength as in prior related work. The spacing in the modified AOA approach can be multiples of the wavelength, which could cause a phase difference of more than 2π.

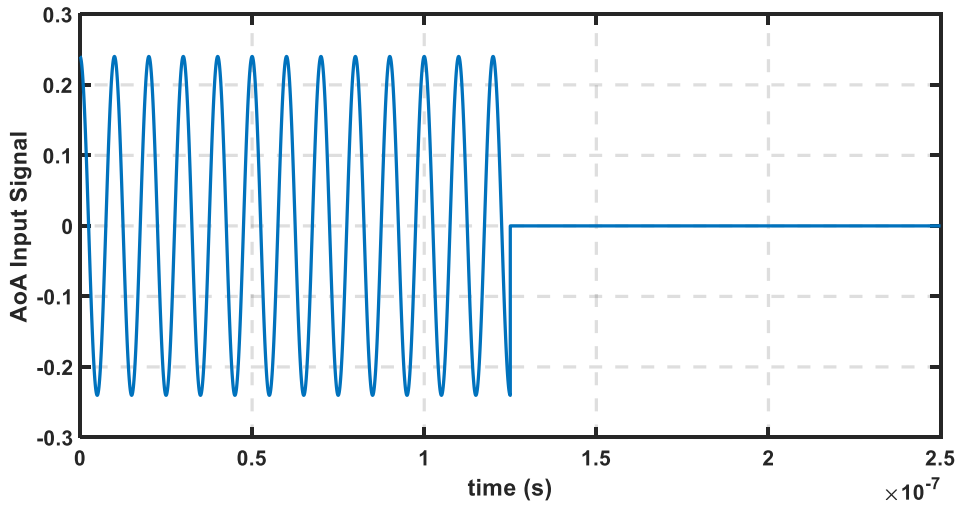

Figure 4.15: AOA input signal at SNR=5.3.

The received signals at each of the three receivers are shown in Fig. 4.16, Fig. 4.17 and Fig. 4.18, respectively.

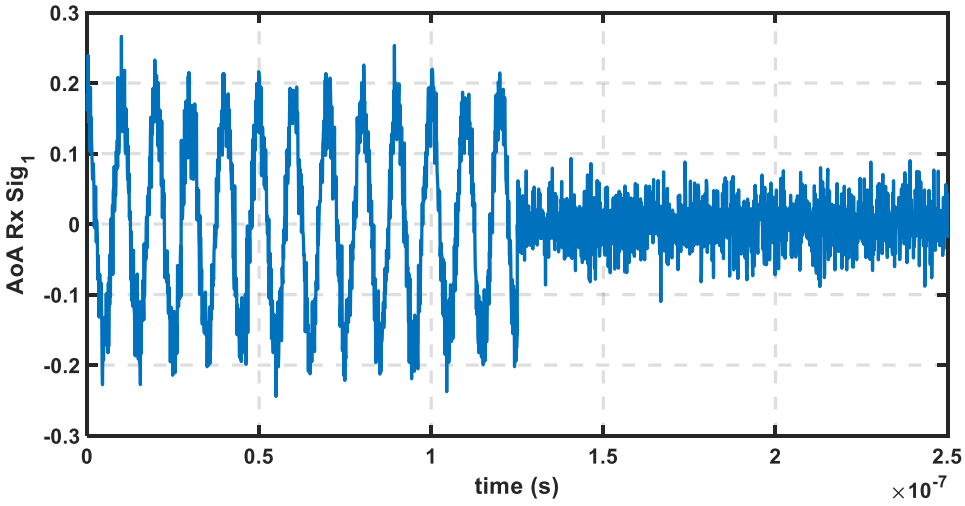

Figure 4.16: AOA received signal at Rx_1 *at* $SNR = 5.3$.

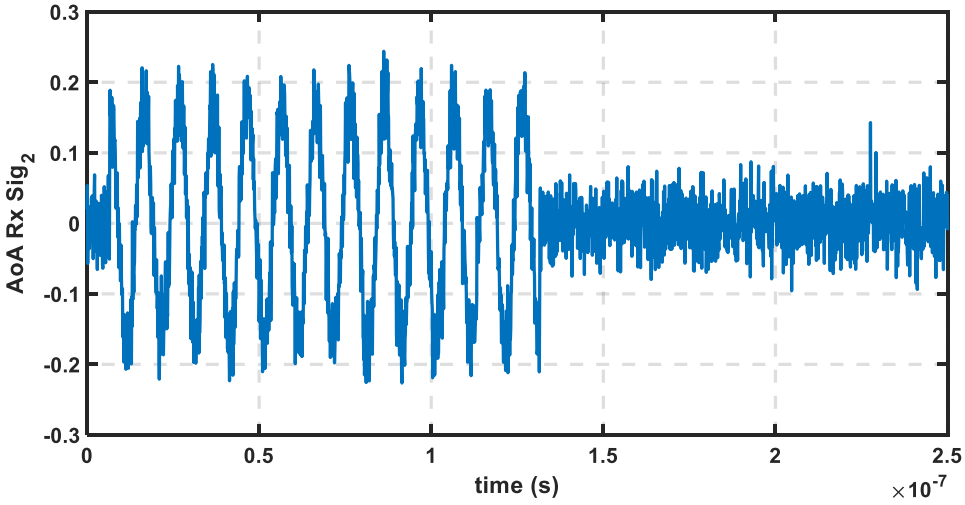

Figure 4.17: AOA received signal at Rx_2 *at* $SNR = 5.3$.

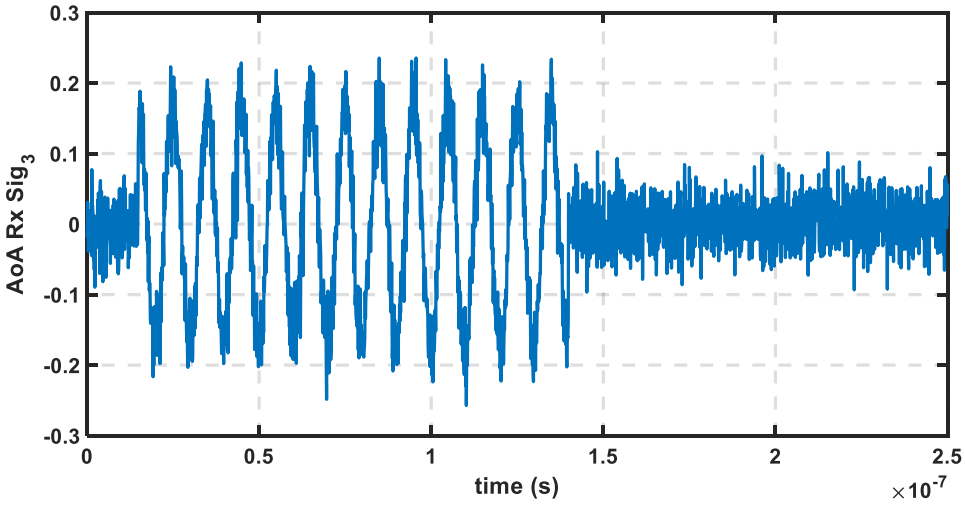

Figure 4.18: AOA received signal at Rx_3 *at* $SNR = 5.3$.

Just like the TDOA approach, the AOA approach is also implemented as a two-step algorithm. In the first step, a 50m × 50m area around the true transmitter coordinates is split into 100 × 100 grid points. At each point the corresponding angles of arrival are calculated using:

$$\theta_{1_{grid}} = \arctan\left(\frac{x_{grid} - x_1}{y_{grid} - y_1}\right) \tag{4.7}$$

$$\theta_{2_{grid}} = \arctan\left(\frac{x_{grid} - x_2}{y_{grid} - y_2}\right) \tag{4.8}$$

$$\theta_{3_{grid}} = \arctan\left(\frac{x_{grid} - x_3}{y_{grid} - y_3}\right). \tag{4.9}$$

The corresponding phase difference elements of the steering vector are calculated using these equations.

$$a(\theta_{1_{grid}},\theta_{2_{grid}}) = \exp\left\{j\frac{2\pi}{\lambda}d\left[\frac{\cos\theta_{2_{grid}}}{\sin(\theta_{2_{grid}}-\theta_{1_{grid}})}(1-\cos(\theta_{2_{grid}}-\theta_{1_{grid}}))-\sin\theta_{2_{grid}}\right]\right\} \quad (4.10)$$

$$a(\theta_{1_{grid}},\theta_{3_{grid}}) = \exp\left\{j\frac{2\pi}{\lambda}2d\left[\frac{\cos\theta_{3_{grid}}}{\sin(\theta_{3_{grid}}-\theta_{1_{grid}})}(1-\cos(\theta_{3_{grid}}-\theta_{1_{grid}}))-\sin\theta_{3_{grid}}\right]\right\} \quad (4.11)$$

$$a(\theta_{2_{grid}},\theta_{3_{grid}}) = \exp\left\{j\frac{2\pi}{\lambda}d\left[\frac{\cos\theta_{3_{grid}}}{\sin(\theta_{3_{grid}}-\theta_{2_{grid}})}\ (1-\cos(\theta_{3_{grid}}-\theta_{2_{grid}}))-\sin\theta_{3_{grid}}\right]\right\} \quad (4.12)$$

Then each element of the steering vector is used to compute the input signal. Since, the transmitted signal is known at the receiver, multiplying each of the steering vector elements by the transmitted signal will generate the corresponding input signal. For example, $a(\theta_{1_{grid}},\theta_{2_{grid}})$ multiplied by transmitted signal yields the first input signal.

$$\mathbf{L}_{AOA} = -\frac{3}{2}\log\ (2\pi\sigma^2) - \frac{\sum_{i=1}^{3}(g_i - h_{i_{grid}}(\theta))^2}{2\sigma^2}. \quad (4.13)$$

The grid that will yield the maximum of $\mathbf{L}_{AOA}$ is the transmitter location.

Fig. 4.19 and Fig. 4.20 show a sample of the estimated x- and y-coordinates at each iteration when SNR=5.3.

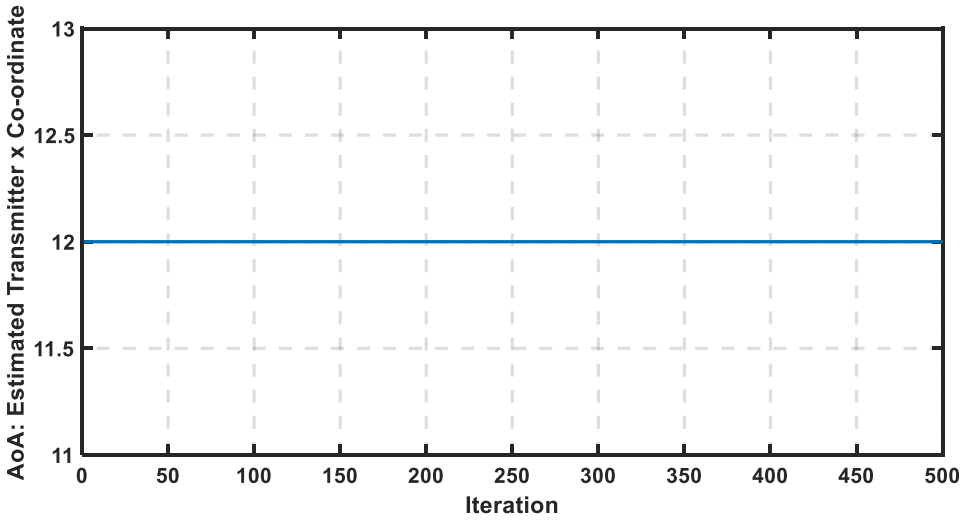

Figure 4.19: AOA approach: Estimated x-coordinate of the transmitter vs. iterations at SNR=5.3.

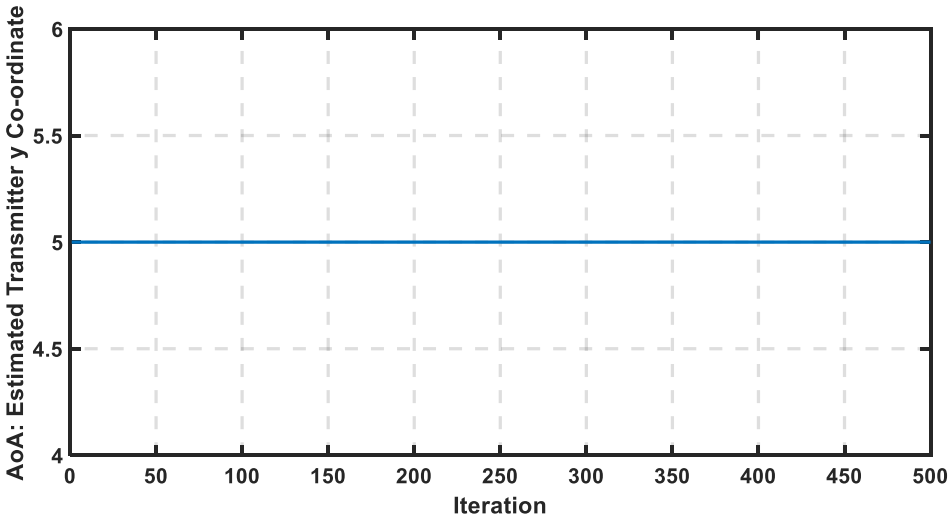

Figure 4.20: AOA approach: Estimated y-coordinate of the transmitter vs. iterations at SNR=5.3.

The results of MSE versus SNR for the x- and y-coordinates are shown in Fig. 4.21 and Fig. 4.22, respectively.

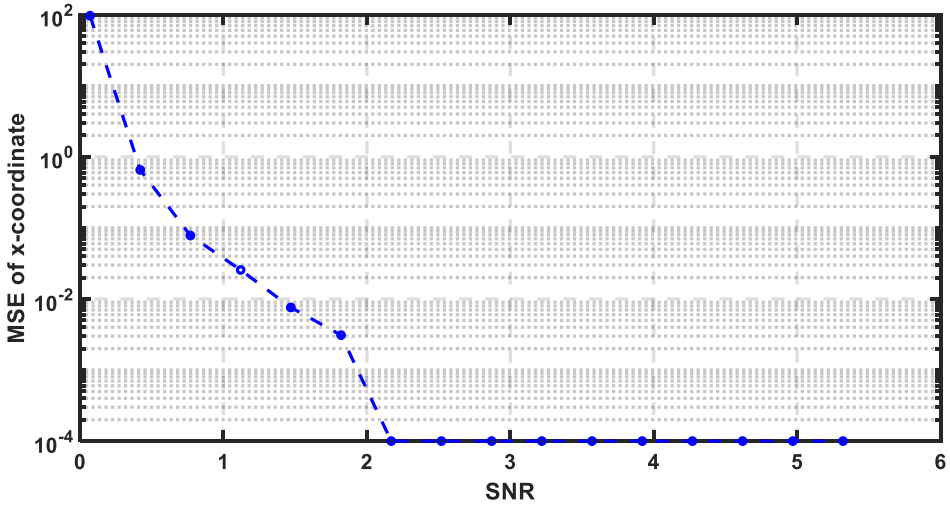

Figure 4.21: AOA approach: MSE vs. SNR for x-coordinate.

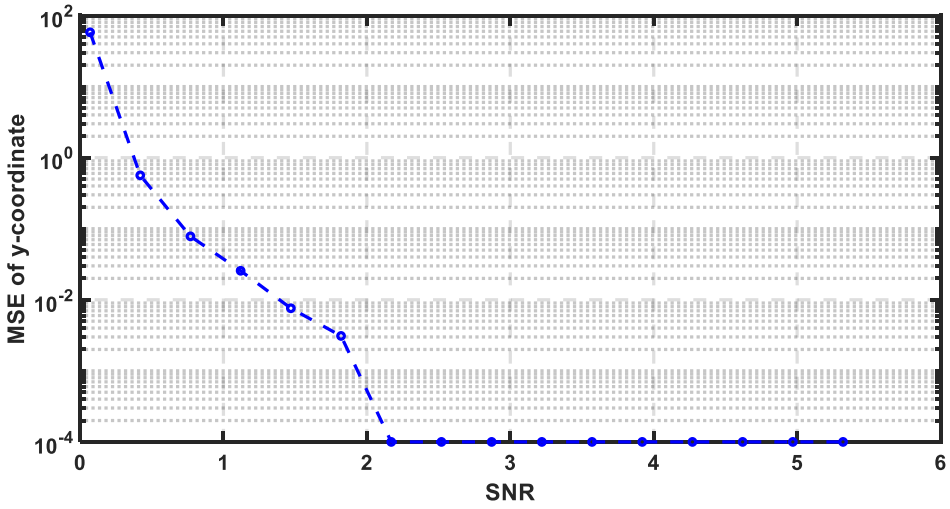

Figure 4.22: AOA approach: MSE vs. SNR for y-coordinate.

As in the TDOA case, the transmitter is restricted to be on half of the plane, that is, the positive y-axis, to eliminate the ambiguity of the mirrored position estimate as discussed for the TDOA case.

Simulation results are obtained for different values of d to show the modified AOA approach performance in each case. The below fig. Figs. 4.23 and 4.24 show the MSE versus SNR when d is set equal to integer multiples of λ.

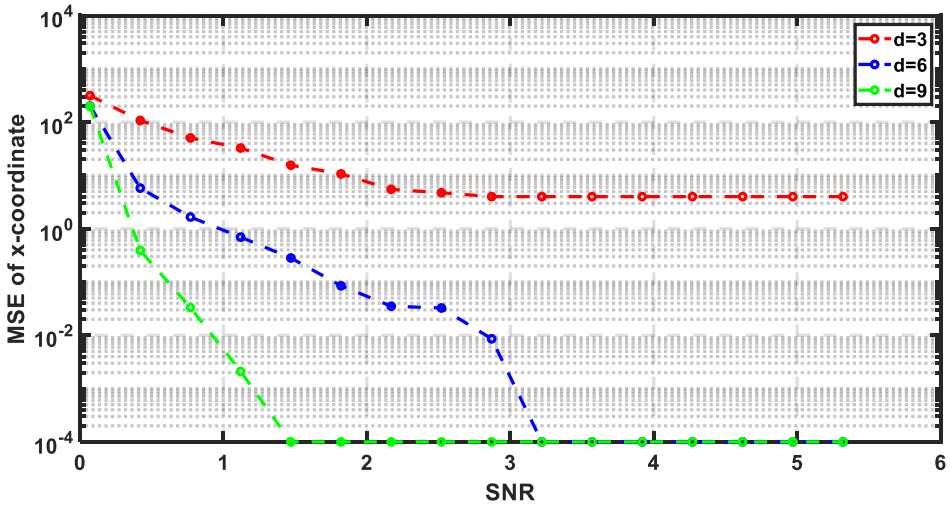

Figure 4.23: Effect of spacing on AOA MSE − x-coordinate.

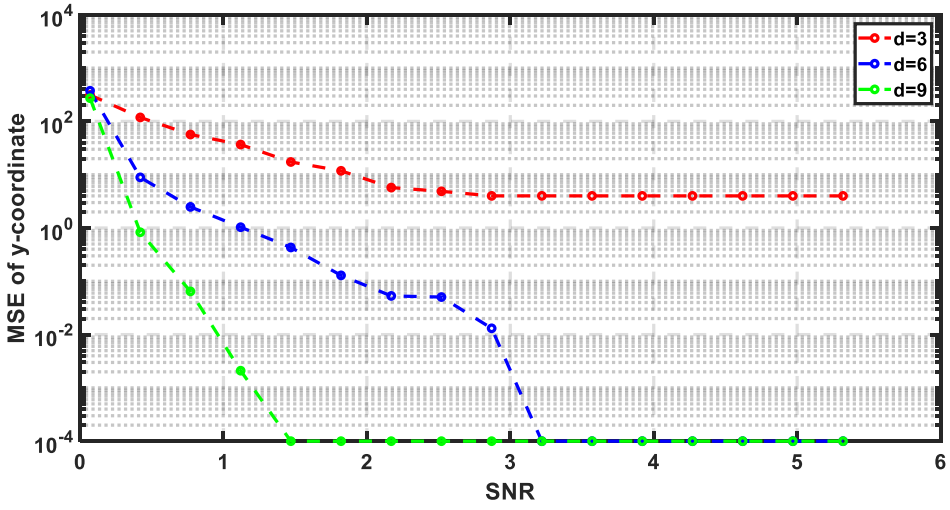

Figure 4.24: Effect of spacing on AOA MSE − y-coordinate.

Figs. 4.23 and 4.24 show that the modified AOA approach implemented does not

require a small spacing between the antennas as the MSE decreases as the antennas spacing increases.

The maximum operating range that AOA approach could cover is another area to be assessed. For this, simulation results are obtained by changing the transmitter location as in TDOA. Figs. 4.25 and 4.26 show the MSE versus SNR for the x- and y-coordinates, respectively.

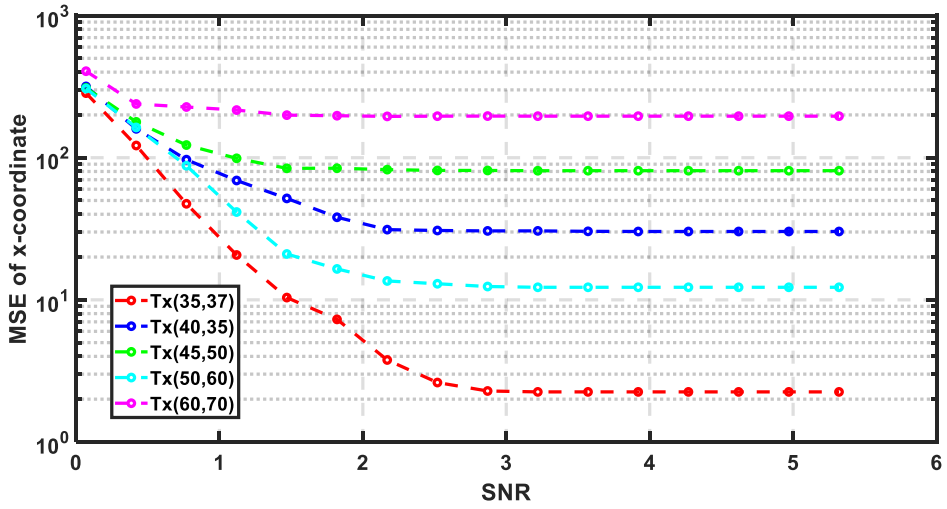

Figure 4.25: AOA approach range – x-coordinate.

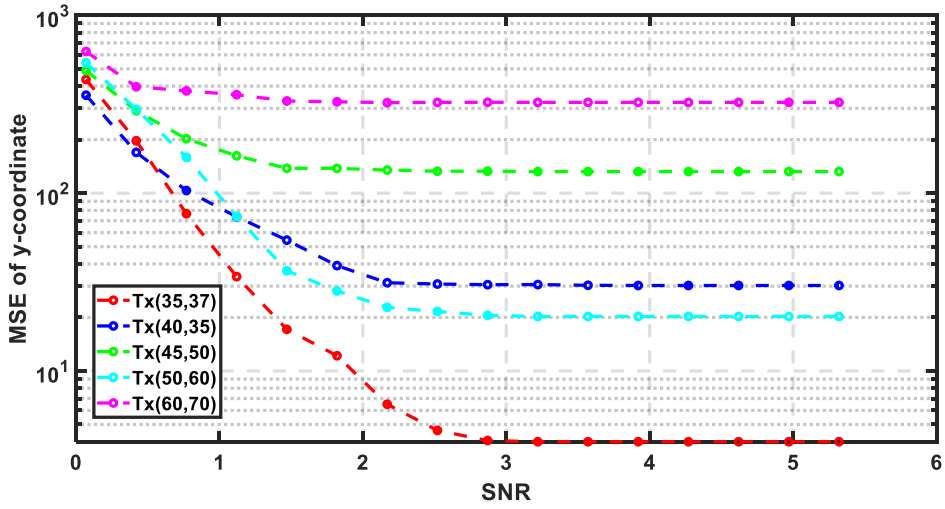

Figure 4.26: AOA approach range − y-coordinate.

Figs. 4.25 and 4.26 show that AOA approach has a wider coverage range than the TDOA approach. The performance is more robust (less MSE) than TDOA when the transmitter is located at the same locations.

4.5 TDOA and AOA Hybrid Solution

Exploiting both schemes to form a hybrid system could potentially extend the coverage range and positioning accuracy. The hybrid method combines the AOAs and TDOAs obtained from the two stand alone systems to get the transmitter coordinate as explained in Sec. 3.4.

Using the two arc points and the coordinates of the first receiver, we sweep an area of 50m × 50m surrounding the true transmitter position as previously done. For each

grid, the three distances to the transmitter are calculated as

$$d_{1t_{grid}} = \sqrt{(x_{grid} - x_1)^2 + ((y_{grid} - y_1)^2} \quad (4.14)$$

$$d_{2t_{grid}} = \sqrt{(x_{grid} - P12_x)^2 + (y_{grid} - P12_y)^2} \quad (4.15)$$

$$d_{3t_{grid}} = \sqrt{(x_{grid} - P13_x)^2 + ((y_{grid} - P13_y)^2}. \quad (4.16)$$

Then, we substitute these distances in the following equation: The grid point that yielded the minimum is the estimated transmitter location. (see Fig. 4.27)

$$f = \mid d_{1t_{grid}} - d_{2t_{grid}} \mid + \mid d_{1t_{grid}} - d_{3t_{grid}} \mid + \mid d_{2t_{grid}} - d_{3t_{grid}} \mid . \quad (4.17)$$

Fig. 4.28 and Fig. 4.29 show examples of the estimated transmitter coordinates at all iterations when SNR=5.3.

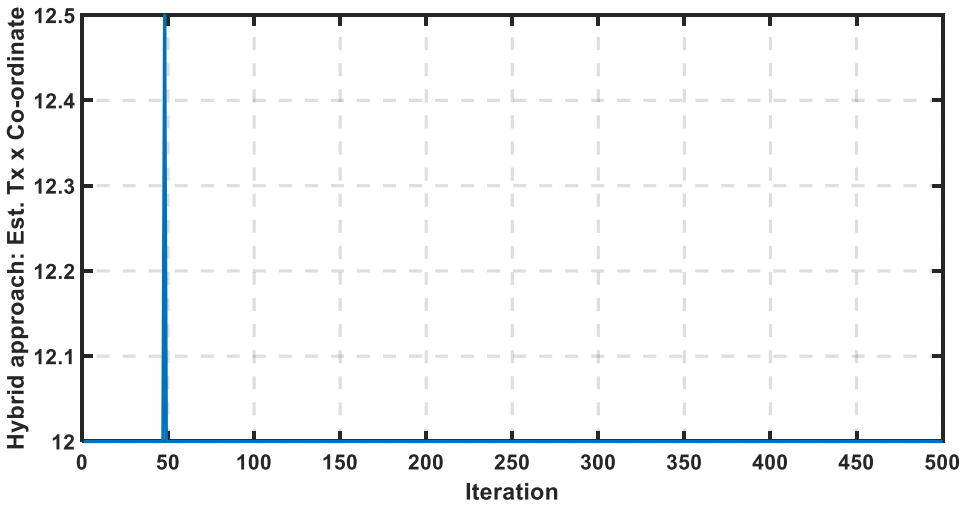

Figure 4.28: Hybrid solution: Estimated x-coordinate of the transmitter vs. iterations.

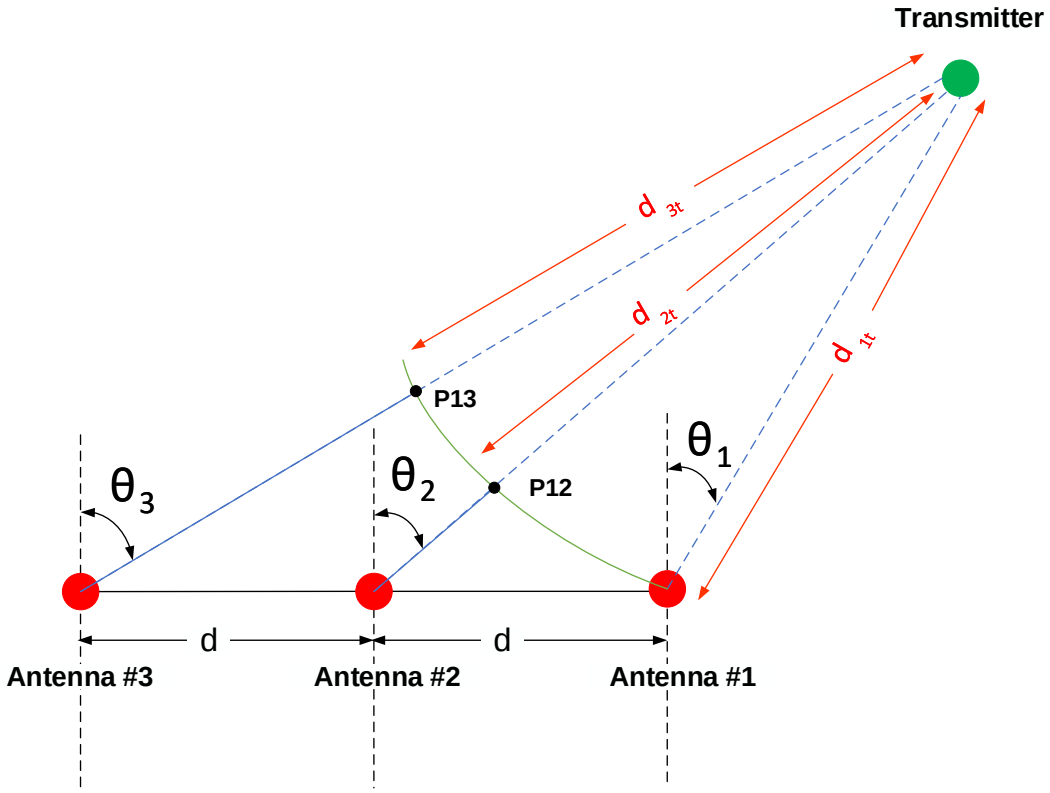

Figure 4.27: Illustration of the distance of transmitter to arc points.

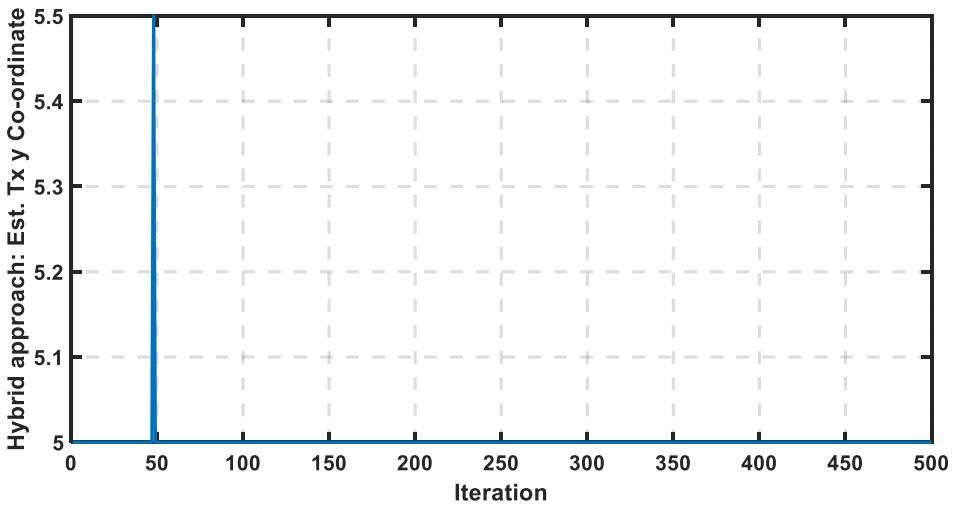

Figure 4.29: Hybrid solution: Estimated x-coordinate of the transmitter vs. iterations.

The MSE versus SNR for each coordinate using the hybrid method is calculated and presented in Fig. 4.30 and Fig. 4.31.

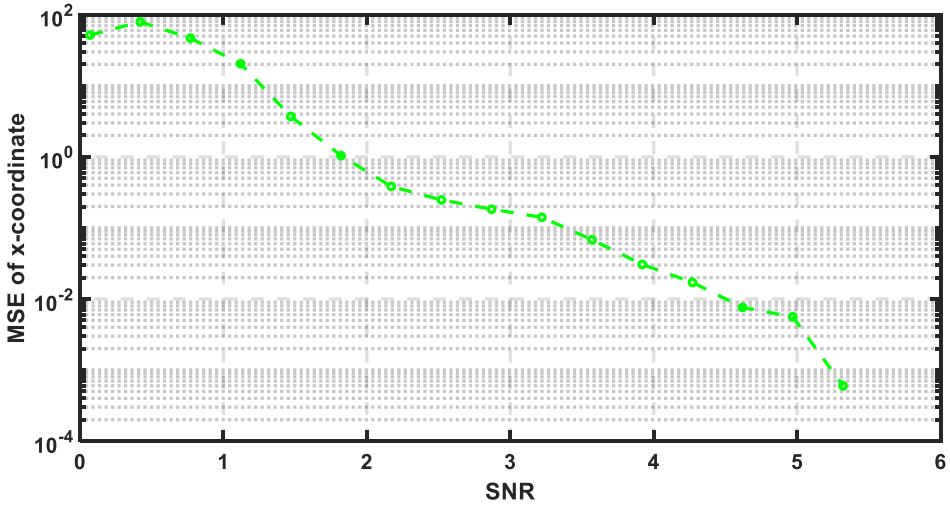

Figure 4.30: Hybrid scheme MSE vs. SNR for x-coordinate.

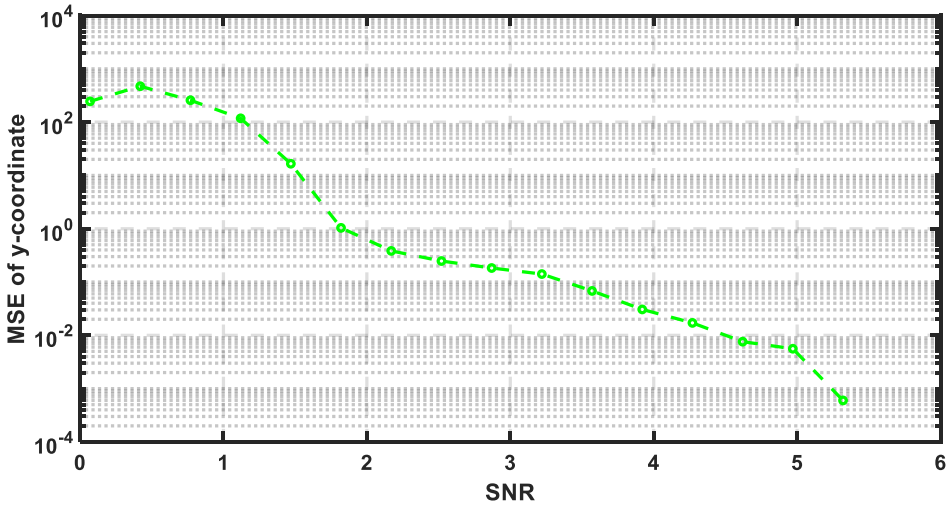

Figure 4.31: Hybrid scheme: MSE vs. SNR for y-coordinate.

The MSE versus SNR values of the three approaches are also presented on a single plot for the transmitter placed at (12,5) in Figs. 4.32 and 4.33.

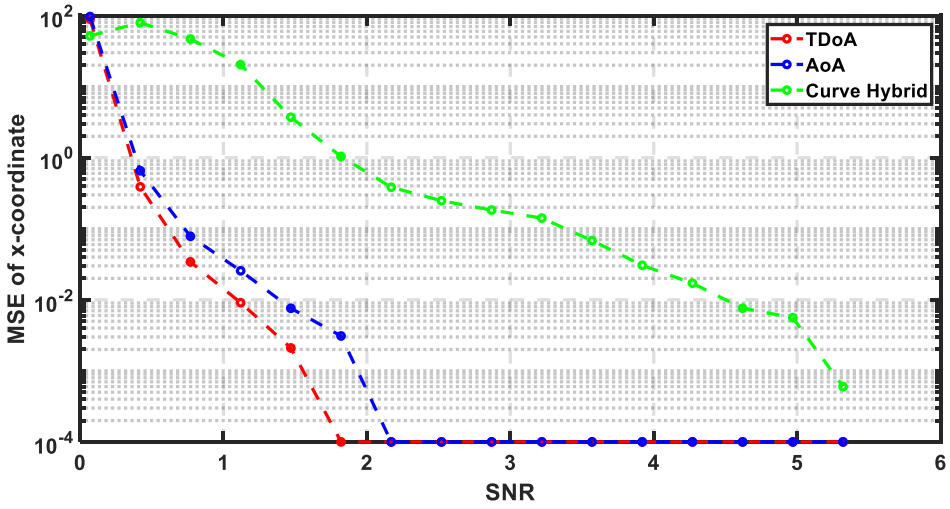

Figure 4.32: All approaches: MSE vs. SNR for x-coordinate for Tx placed at (12,5).

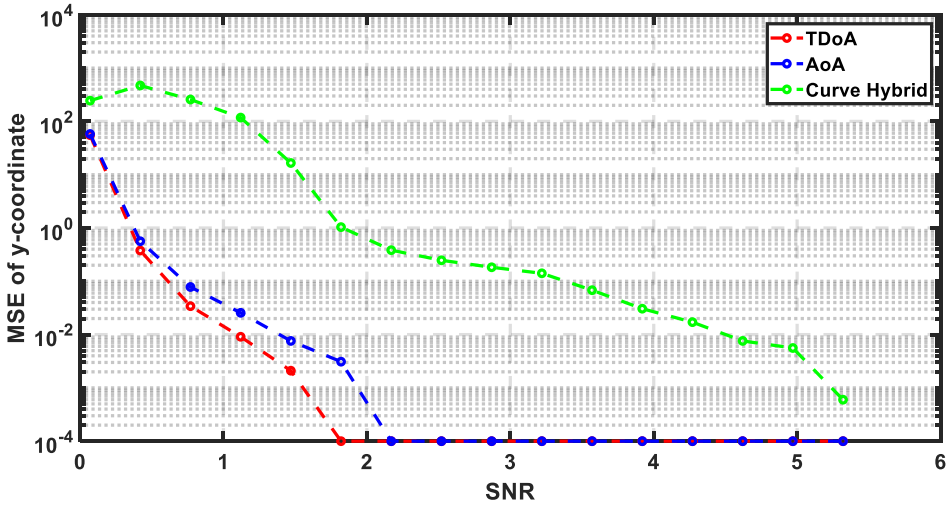

Figure 4.33: All approaches: MSE vs. SNR for y-coordinate for Tx placed at (12,5).

It can be concluded from Fig. 4.32 and Fig. 4.33 that the TDOA approach has the

best MSE when the transmitter was placed at (12,5).

We run the same set of simulations after changing only the transmitter location to (60,70). The results of the MSE versus SNR for all the three approaches are shown in Figs. 4.34 and 4.35.

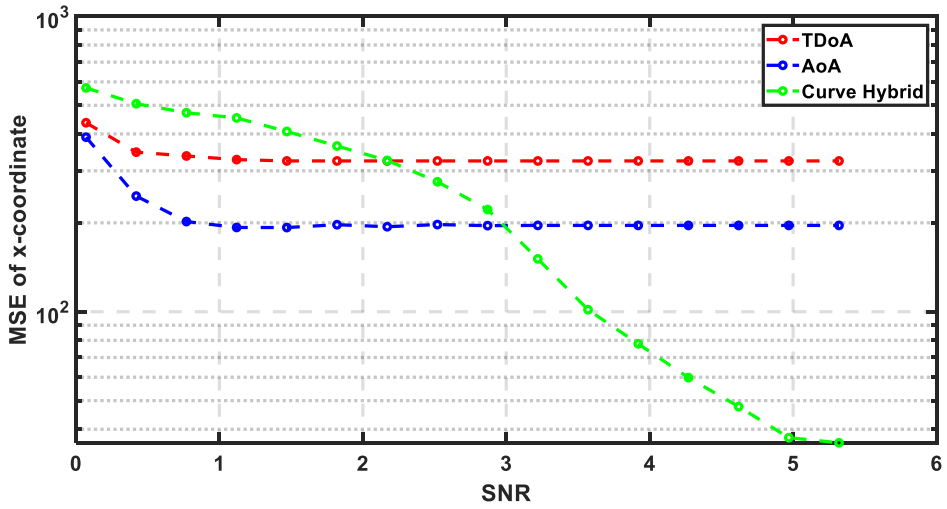

Figure 4.34: All approaches: MSE vs. SNR for x-coordinate for Tx placed at (60,70).

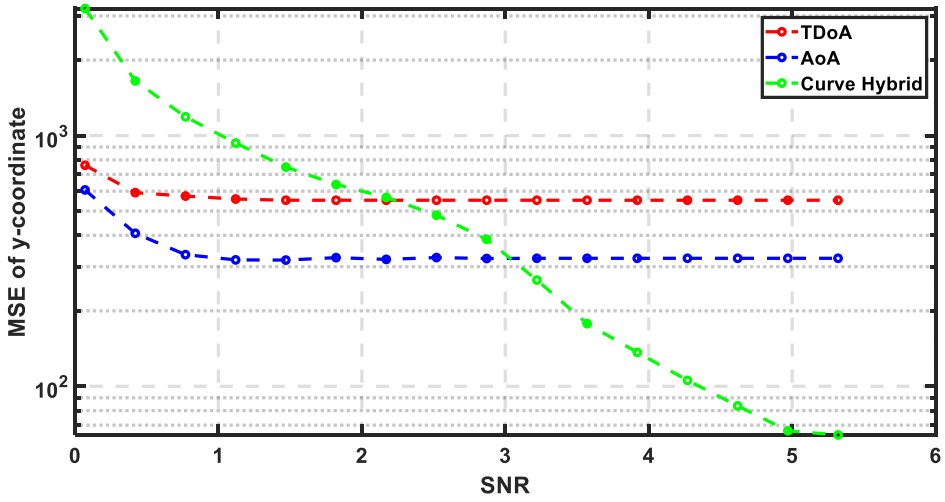

Figure 4.35: All approaches: MSE vs. SNR for y-coordinate for Tx placed at (60,70).

Figs. 4.34 and 4.35 show that the hybrid approach generates a lower MSE than any of the stand alone approaches when transmitter is far away from the transmitter at (40,40).

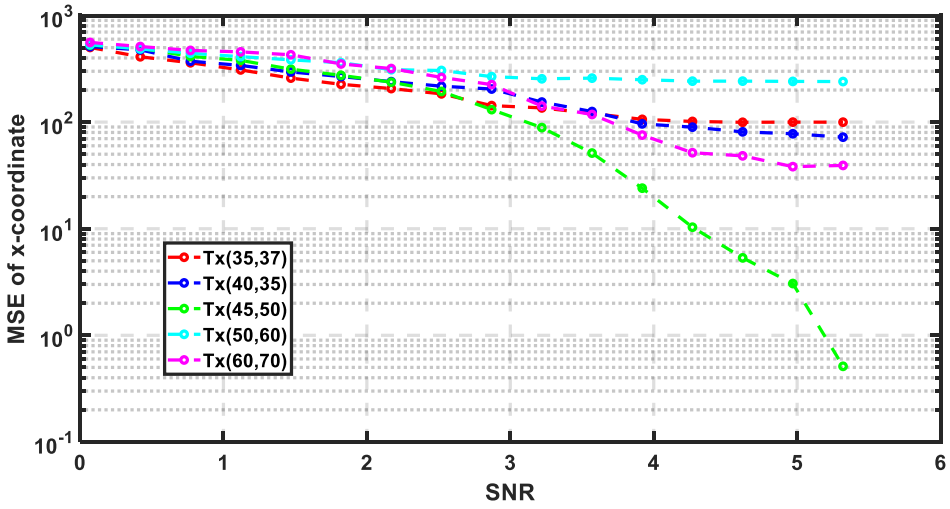

Figure 4.36: Hybrid approach range − x-coordinate.

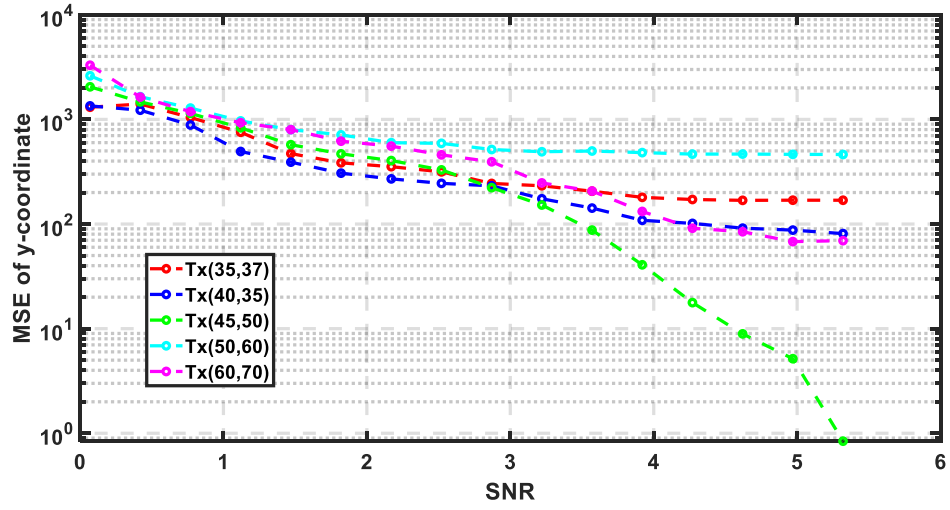

Figure 4.37: Hybrid approach range − y-coordinate.

Fig. 4.36 and 4.37 show the results of the same study TDOA and AOA approaches.

These results show that the hybrid method has better MSE when the transmitter is placed far from the antennas array than when it is close to it.

4.6 Reconfigurability

On of the advantages of the proposed system is that it is easily reconfigurable. In order to increase the coverage range, we can add an appropriate number of receiving antennas, and it is unnecessary to change any of the existing components.

The simulation results in Figs. 4.38 and 4.39 provide a comparison between the MSE versus SNR plots when the transmitter is located at (20.5,8.5) in two scenarios: with three receiving antennas and with four receiving antennas.

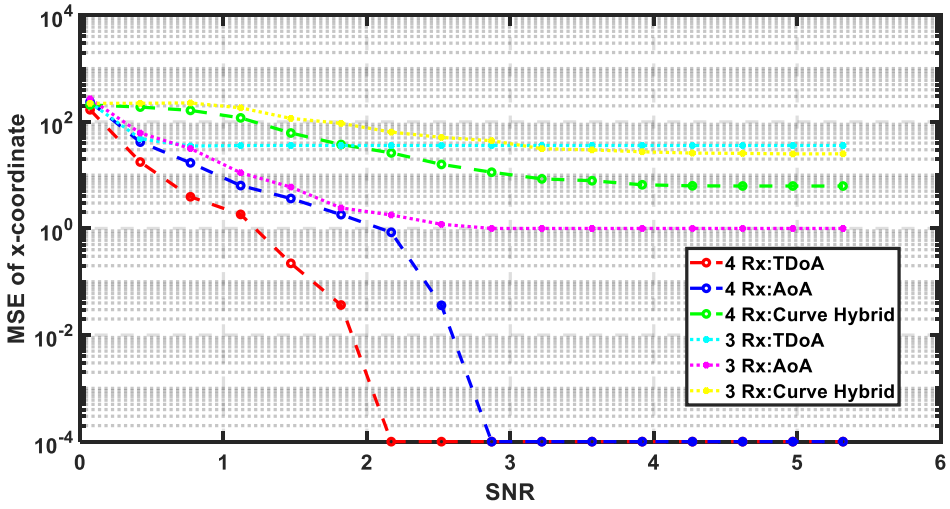

Figure 4.38: Comparison between 3 receivers and 4 receivers at $d = 3$ and Tx location (20.5,8.5) $-$ x-coordinate.

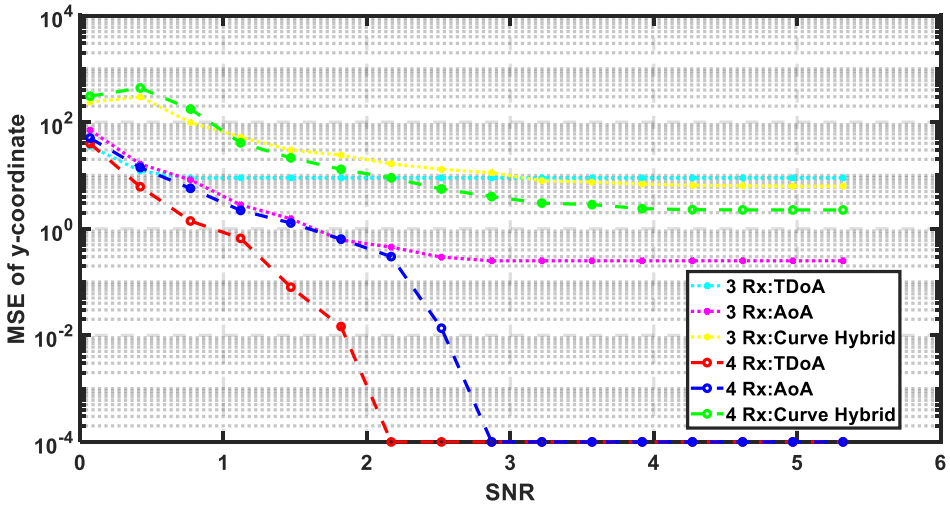

Figure 4.39: Comparison between 3 receivers and 4 receivers at $d = 3$ and Tx location (20.5,8.5) – y-coordinate.

These results show that adding receivers will increase the system coverage range as expected.

Chapter 5: Conclusion and Discussion

A hybrid TDOA-AOA positioning system is proposed, aiming to provide a very simple structure with a single linear array of receivers while still maintaining a good performance. The TDOA scheme has the best MSE results for small ranges AOA has the best MSE results for medium ranges. They are best used for 'near field' systems. The hybrid method has the best MSE results when the transmitter is far away from the receiver array. The proposed system is efficient as it has a large coverage range with low computation required. It is flexible, there is no limitation on the transmitter location. It can be easily reconfigured without having to change existing installation and it is cost effective.

In summary, a reconfigurable positioning system that can use three different approaches– TDOA, AOA, and hybrid scheme has been implemented. The spacing between the antennas on the receiver array can be flexibly chosen. Coverage area and performance can be flexibly traded-off with the number of receiving antennas on the array.

More work needs to be done by including a good model of the multipath fading channel. Additionally new methods that do not rely on area sweeping to find the solutions will reduce the computational complexity.

Bibliography

[1] R. Ye, S. Redfield, and H. Liu, "High-precision indoor UWB localization: Technical challenges and method," in *Proc. IEEE ICUWB'10*, Nanjing, China, Sep. 2010.

[2] Y. Zou, H. Liu, W. Xie, and Q. Wan, "Semidefinite programming methods for alleviating sensor position error in TDOA localization," *IEEE Access*, vol. 5, pp. 23111–23120, Sep. 2017.

[3] T. Qiao and H. Liu, "Improved least median of squares localization for non-line-of-sight mitigation," *IEEE Communications Letters*, vol. 18, no. 8, pp. 141-144, Aug. 2014.

[4] T. Qiao and H. Liu, "An improved method of moments estimator for TOA based localization," *IEEE Communications Letters*, vol. 17, no. 7, pp. 1321–1324, Jul. 2013.

[5] T. Qiao, S. Redfield, A. Abbasi, Z. Su, and H. Liu, "Robust coarse position estimation for TDOA localization," *IEEE Wireless Communications Letters*, vol. 2, no. 6, pp. 623–626, Dec. 2013.

[6] Z. Su, G. Shao, and H. Liu, "Semidefinite programming for NLOS error mitigation in TDOA localization," *IEEE Communications Letters*, vol. 22, no. 7, pp. 1430-1433, July 2018.

[7] Y. Zou, H. Liu, and Q. Wan, "Joint synchronization and localization in wireless sensor networks using semidefinite programming," *IEEE Internet of Things Journal*, vol. 5, no. 1, pp. 199–205, Feb. 2018.

[8] Y. Zou, H. Liu, and Q. Wan, "An iterative method for moving target localization using TDOA and FDOA measurements," *IEEE Access*, vol. 6, pp. 2746-2754, Feb. 2017.

[9] Y.-T. Chang, "Simulation and implementation of an integrated TDOA/AOA monitoring system for preventing broadcast interference," *Journal of Applied Research and Technology*, vol. 12, no. 6 pp. 1051–1062, 2014.

[10] Y. T. Chang and Y.-C. Lin, "Implementation and experiments of TDOA monitoring techniques for broadcasting interferences," *Applied Mechanics and Materials*, vol. 479, pp.996–1000, 2014.

[11] M. A. C. Duran, A. A. D'Amico, D. Dardari, M. Rydström, F. Sottile, E. G. Ström, and L. Taponecco, "Terrestrial network-based positioning and navigation," *Satellite and Terrestrial Radio Positioning Techniques*, pp. 75-153, 2012.

[12] P. Gupta and S. P. Kar, "Music and improved music algorithm to estimate direction of arrival," in *Proc. 2015 Int. Conf. Communications and Signal Processing (ICCSP)*, pp. 757-761, Apr. 2015.

[13] S. M. Kay. *Fundamentals of statistical signal processing.* Prentice Hall PTR, 1993.

[14] R. Qiu, H. Liu, and S. Shen, "Ultra-wideband for multiple-access communications," *IEEE Communications Magazine*, vol. 43, no. 2, pp. 80-87, Feb. 2005.

[15] H. Liu, "Error performance of a pulse amplitude and position modulated ultra-wideband system in lognormal fading channels," *IEEE Communications Letters*, vol. 7, no. 11, pp. 531-533, Nov. 2003.

[16] H. Liu, R. Qiu and Z. Tian, "Error performance of pulse-based ultra-wideband MIMO systems over indoor wireless channels," *IEEE Transactions on Wireless Communications*, vol. 4, no. 6, pp. 2939-2944, Nov. 2005.

[17] H. Liu, "Multicode ultra-wideband scheme using chirp waveforms," *IEEE Journal on Selected Areas in Communications*, vol. 24, no. 4, pp. 885-891, Apr. 2006.

[18] S. Zhao, H. Liu, and Z. Tian, "Decision directed autocorrelation receivers for pulsed ultra-wideband systems," *IEEE Transactions on Wireless Communications*, vol. 5, no. 8, pp. 2175-2184, Aug. 2006.

[19] S. Zhao, H. Liu, and Z. Tian, "A decision-feedback autocorrelation receiver for pulsed ultra-wideband systems," in *Proc. IEEE Radio and Wireless Conf.*, pp. 251-254, Sep. 2004

[20] S. Zhao and H. Liu, "On the optimum linear receiver for impulse radio systems in the presence of pulse overlapping, *IEEE Communications Letters*, vol. 9, no. 4, pp. 340-342, Apr. 2005.

[21] S. Zhao and H. Liu, "Transmitter-side multipath preprocessing for pulsed UWB systems considering pulse overlapping and narrow-band interference," *IEEE Transactions on Vehicular Technology,* vol. 56, no. 6, pp. 3502-3510, Nov. 2007.

[22] S. Zhao, P. Orlik, A.F. Molisch, H. Liu, and J. Zhang "Hybrid ultrawideband modulations compatible for both coherent and transmit-reference receivers," *IEEE Transactions on Wireless Communications*, vol. 6, no. 7, pp. 2551-2559, July 2007.

[23] S. Zhao and H. Liu, "Prerake diversity combining for pulsed UWB systems considering realistic channels with pulse overlapping and narrow-band interference," in *IEEE Global Telecommunications Conference*, Nov. 2005.

[24] R. Ardoino and F. Capriati. "DTOA estimation of pulse trains by means of cross-correlation technique," in *Proc. 2008 IEEE Radar Conference*, pp. 1–6, 2008.

[25] A. Patwari and G. R. Reddy, "1D direction of arrival estimation using root-music and esprit for dense uniform linear arrays," in *Proc. 2017 2nd IEEE Int. Conf. Recent Trends Electronics, Information Communication Technology (RTEICT)*, pp. 667–672, May 2017.

[26] M.P. Priyadarshini and R. Vinutha, "Comparative performance analysis of music and esprit on ULA," in *Proc. 2012 IEEE Int. Conf. Radar, Communication and Computing (ICRCC)*, pp. 120–124, 2012.

[27] R. Schmidt, "Multiple emitter location and signal parameter estimation," *IEEE Transactions on Antennas and Propagation*, vol. 34, no. 3, pp. 276–280, Mar. 1986.

[28] B. Tay, W. Liu, and D. H. Zhang, "Indoor angle of arrival positioning using biased estimation," in *Proc. 2009 7th IEEE Int. Conf. Industrial Informatics*, pp. 458–463, 2009.

[29] D. J. Torrieri, "Statistical theory of passive location systems," *IEEE Transactions on Aerospace and Electronic Systems*, vol. AES-20, no. 2, pp. 183–198, Mar. 1984.

[30] N. Vankayalapati, S. Kay, and Q. Ding. "TDOA based direct positioning maximum likelihood estimator and the cramer-rao bound," *IEEE Transactions on Aerospace and Electronic Systems*, vol. 50, no. 3, vol. 1616–1635, Jul. 2014.